UNIVERSIDADE DE LISBOA
FACULDADE DE CIÊNCIAS
DEPARTAMENTO DE BIOLOGIA VEGETAL

An investigation of cell cycle regulation during in vitro models of diapause

Andreia Almeida

Mestrado em Biologia Molecular e Genética

Dissertação Orientada por:
Dr. Harry Leitch
Prof. Gabriela Rodrigues

2021

Acknowledgements

Para a minha família:

Obrigada a todos os de longe (avô e irmã) e aos de perto (mãe e irmã) por todo o apoio e confiança. Por me ajudarem realizar este desejo de ir para fora e ter esta experiência única. Obrigada!

To my friends:

Thank you Inês for being there unconditionally since the beginning. For hearing and supporting me when I needed. For neutralize and laugh with me about all the challenges. And for always giving the other point of view, in both daily bases and science situations.

Rafaela, thank you for the moments of mutual frustration sharing. Thanks for listening as well, for being such a cutie and an example as always!

To Prof. Gabriela Rodrigues, thank you for your availability to be my supervisor, as well as for your kindness along the project.

To *Both Labs*:

I would like to express my gratitude to Harry Leitch and Alexis Barr for accepting me in the lab, giving me the opportunity of doing my Master thesis project at the MRC - London Institute of Medical Sciences, which was an extremely enriching experience. And specially, thanks for proposing a very interesting project! Also, thank you for all the help and suggestions during the project. And not least, at all... thank you for all the social and funny moments that made my experience in London much better.

Gosia and Steve, thank you for all the introductions. Thank you, a lot, to both of you (Or should I give tons of coffee/beer instead?)!

Daichi, thank you for all the tips. For being my quick hero in some mini panic moments, plus for being my mouse cells buddy. Thanks.

Irina, my office girl buddy, thank you for the support and fun chats.

Thank you Lessly, Beth, Camille, Jordan, Lucas and Keir and all the second-floor people for all the little big helps. For the daily support, lunches and company, that basically made the LMS and London feel like home.

To Twenty, the black cat, that during the results analysis and writing processes gave the biggest help and company.

P.s- Thanks to the city of London. Although Covid, TFL and the weather weren't fun, London still has my heart after more than a year. Thanks for receiving me!

Resumo

Durante o desenvolvimento embrionário, as células do embrião dão origem a diferentes tecidos, dependendo da potência que tiverem. Em estados iniciais do desenvolvimento embrionário, as células pluripotentes surgem no epiblasto (EPI), pré-implantação. Estas células têm a capacidade de formar qualquer tipo de linha celular das três camadas germinativas, e ainda as células germinais primitivas. As células pluripotentes de ratinho podem ser isoladas da massa celular interna do blastocisto (estágio 3.5) e mantidas *in vitro*, com a capacidade de se dividirem e renovarem-se a si próprias, em um meio condicionado chamado 2i/LIF. Estas células são chamadas de células estaminais embrionárias de rato, com a sigla mESCs (vinda do inglês "mouse embryonic stem cells"). Ainda durante o início do desenvolvimento, os embriões de várias espécies de mamíferos podem entrar num estado de dormência, conhecido como diapausa. Diapausa é caracterizado pelo atraso da implantação do embrião às paredes uterinas. Estudos mostram que este estado é induzível *in vitro* tanto em blastocistos (pela inibição da hormona estrogénio e injeção diária de progesterona), como em mESCs (pela inibição da molécula mTOR ou da c-Myc). *In vivo*, após cinco dias da indução da diapausa, foi sugerido que as células da massa celular interna do blastocisto têm um metabolismo semelhante ao dos estados de quiescência. Quiescência é um tipo de paragem do ciclo celular, reversível, que em muitas espécies é semelhante com diapausa. Um exemplo de quiescência foi demonstrado ser provocado após acumulação da proteína p21, em resposta a danificação intrínseca do ADN. Em blastocistos nos quais a diapausa foi induzida, foi sugerido que p21 medeia a retenção das células do blastocisto na fase G0/G1 do ciclo celular e que reduz a replicação do ADN. Apesar disto, ainda não é conhecido se o ciclo celular das mESCs em diapausa é suspenso ou se o seu progresso é desacelerado. Por tanto, ainda não se sabe se este processo é dependente da proteína p21 e/ou se tem outro mecanismo envolvido.

O objetivo do meu projeto é caracterizar a regulação do ciclo celular em mESCs, *in vitro*, e como é iniciado, mantido e terminado o estado de diapausa. Para tal, técnicas de quantificação de imagens de células tanto fixadas como vivas foram usadas para avaliar a expressão de reguladores do ciclo celular. Foi ainda desenvolvido uma linha celular que reporta a atividade de p21 com fluorescência, por CRISPR/Cas9. O avanço do nosso conhecimento nesta área poderá permitir a confirmação de se diapausa ocorre em humanos, em estudos futuros, possivelmente permitindo uma melhor previsão das datas de nascimento. Por outro lado, este avanço poderá ainda informar o nosso conhecimento para descoberta de novas terapias oncológicas, visto que alguns cancros parecem resistir a quimioterapia através da entrada num estado semelhante a diapausa.

Aqui, foi reproduzido o modelo de dormência, antes publicado, pela inibição de mTOR (mTORi). Este modelo foi usado para explorar o fenótipo do seu ciclo celular. Através dele, observou-se que o mTORi também causa suspensão do progresso do ciclo celular, com a redução da fração de células que estão na fase S do ciclo, aumento das células em G1, e ainda redução dos valores de expressão da proteína ciclina D e da fosforilação da proteína Rb (P-Rb). Resultados semelhantes foram obtidos quando Nutlin foi usada como tratamento, um ativador da proteína p53. Este tratamento também reduziu o crescimento das mESCs, e a fração de células na fase S. No entanto, os valores de fluorescência de P-Rb quando Nutlin é usado sugerem duas populações de células. Quando o ciclo celular destas células tratadas foi analisado, observou-se um aumento da percentagem de células tanto na fase G1 como na G2, sugerindo que a divisão em subpopulações indicadas pelos níveis de P-Rb poderá ser devido a estarem suspensas em fases diferentes do ciclo celular. Adicionalmente, demonstrou-se ainda que mESCs são menos sensíveis a tratamento que inibem CDK4/6, como Palbociclib, em relação a células somáticas. Palbociclib reduziu os níveis de P-Rb e a fração de células da fase S, com o aumento de células em G1. Contrariamente aos outros inibidores usados, com Palbociclib não se observou alterações nas intensidades detetadas da proteína ciclina D.

Adicionalmente, com o intuito de acompanhar a dinâmica dos níveis de expressão da proteína p21, em tempo real, enquanto as células entravam e saiam do estado de diapausa, as mESCs foram transfetadas para incorporar o ADN da proteína de fluorescência mRuby, dentro do gene que codifica a proteína p21, usando CRISPR/Cas9.

Posto isto, o relatório final do projeto está aqui representado, apontando novos conhecimentos fascinantes e pontos importantes para próximos estudos, na investigação de como as mESCs entram e saem do estado de diapausa.

Palavras-chave: mESCs, dormência, quiescência, p21, cancro

Abstract

During embryonic development cells can give rise to different tissues, depending on their potency. Early in embryonic development, pluripotent cells emerge in the pre-implantation epiblast (EPI) which have the capacity to form any cell type derived from one of three primary germ cell layers, as well as germ cells. Mouse pluripotent cells can be isolated from the EPI (embryonic day (E)4.5) and maintained *in vitro* as self-renewing mouse embryonic stem cells (mESCs) in a culture medium called 2i/LIF. Also, early in development, mammalian embryos of various species can go through a dormancy stage, known as diapause, which in mouse is characterized by a delay in blastocyst implantation. This stage has been induced *in vitro* either in blastocysts or in mESCs by inhibition of oestrogen and daily progesterone injection, or inhibition of c-Myc or mTOR, respectively. *In vivo*, after five days of diapause induction, it has been suggested that inner cell mass (ICM) cells are metabolically quiescent. Quiescence is a reversible cell cycle arrest that, in many aspects, appears similar to diapause. One example of quiescence is due to accumulation of p21 in response to intrinsic DNA damage. In diapaused blastocysts *in vitro,* it has been suggested that p21 mediates the retainment of the blastocyst's cells in G0/G1-phase and DNA replication reduction during diapause. Despite these findings, in diapaused mESCs it is still poorly understood whether the cells are arrested in a particular cell cycle phase or only present a slower proliferation rate. Therefore, it is unclear if this process is p21-dependent and/or if other molecular mechanisms are involved.

The aim of my project is to characterize how the cell cycle of mESCs is regulated *in vitro* and how they enter, maintain and exit diapause. For this, quantitative fixed and live cell imaging was used to evaluate the expression of cell cycle regulators, and I developed a fluorescent reporter of p21 activity, engineered by CRISPR/Cas9. Advancing our knowledge in this area may permit further studies to confirm if diapause occurs in human, by comparing cell cycle regulations between mESCs with hESCs, that may lead to adjusted pregnancy dates. Alternatively, this might provide insight to cancer therapies, since some cancers might resist chemotherapy by entering into a diapause-like state.

Here, I reproduce a published model of dormancy using inhibition of mTOR (mTORi). I used this model to explore cell cycle phenotypes and observed that treatment with mTORi also shows cell cycle arrest with a reduction in the fraction of S-phase cells, increase of cells in G1-phase, reduced Cyclin D levels and a reduction of Rb phosphorylation. Similar results were obtained with the p53 activator Nutlin. Nutlin caused reduced growth in mESCs, and a reduction in the fraction of S-phase cells. However, staining for P-Rb following Nutlin treatment suggest two populations of cells. Cell cycle analysis of Nutlin treated cells showed an increase of cells in both G1- and G2- phases. This may suggest that different P-Rb subpopulations are formed depending on which stage of the cell cycle they arrest in. I also show that mESCs are less sensitive to the CDK4/6 inhibitor Palbociclib than somatic cells. Palbociclib also reduces the percentage of mESCs in S-phase, with an increase of cells in G1-phase, reduction of Rb phosphorylation and, in contrast with the other treatments, I observed no change in Cyclin D intensity.

In addition, in order to track p21 expression dynamics in real-time as cells enter and exit diapause states, I transfected mESCs to incorporate mRuby DNA (red fluorescence protein) within the p21 coding gene, by CRISPR/Cas9.

Taken together this improves our understanding of cellular quiescence and points towards next steps in the investigation of how mESCs enter and exit a diapause-like state.

Keywords: mESCs, dormancy, quiescence, p21, cancer

Contents

List of Figures

List of Tables

List of Abbreviations

°C – Celsius

µg – Micrograms

µL – Microliter

µmol – Micromole

% - Percentage

2i/LIF - Medium with the two inhibitors – PD and CHIR – plus LIF for maintenance of pluripotency.

Ab – Antibodies

bp – Base pairs

BSA - Bovine serum albumin

CAK - CDK-activating kinase

cdc25 - Cell division cycle 25 protein

CDK1/2i – CDK1/2 III inhibitor

CDKIs - Cyclin-dependent kinase inhibitors, CDKs complexes' negative regulators.

Cdkn1a – gene encoding p21 protein

CDKs - Cyclin-dependent kinases

cDNA - Complementary deoxyribonucleic acid

CHIR - CHIR99021 is an aminopyrimidine derivative that inhibits glycogen synthase kinase-3

CL medium – CH + LIF medium

c-Myci - Inhibitor (10058-F4) of c-Myc (transcription factor), prevents c-Myc-Max dimerization and transactivation of c-Myc target gene expression

CRISPR/Cas9 - clustered regularly short palindromic repeats-CRISPR associated nucleases

Cycs - Cyclins

DNA - Deoxyribonucleic acid

DMEM/F12 - Dulbecco's Modified Eagle's Medium/F-12

DMSO - Dimethyl Sulfoxide

DSB - Double strand breaks

E14 - E14Tg2A cell line, Morita et al. 2000

E2F - Transcription factor

ECs - Embryonic carcinomas

EdU - 5-ethynyl-2'-deoxyuridine

EPI - Pre-implantation epiblast

EpiLCs - Epiblast-Like cells

EpiSCs - Primed epiblast stem cells

ESCs - Embryonic stem cells

FACS - Fluorescence-activated cell sorting

FGF - Fibroblast growth factor

FSCs - Formative stem cells

gDNA - Given deoxyribonucleic acid

gRNA – Guide ribonucleic acid

h – Hour

hESC - Human embryonic stem cells

IC_{50} – Inhibitory concentration for 50 % of the required effect

ICM - Inner cell mass

iPSCs - Induced pluripotent stem cells

IUGR - Intra uterine growth restriction

IVF - *In vitro* fertilisation

kDa - Kilo Dalton

LB - Luria Bertani medium

LIF - Leukaemia inhibitory fator

M - Molar

MEFs - Mouse embryonic feeders

mESCs - Mouse embryonic stem cells

min - Minute

mL - Mililiter

mM - Milimolar

mPSCs - Mouse pluripotent stem cells

mTORi - INK-128 that inhibits m-TOR (also called FRAP1, is a member of the phosphatidylinositol 3-kinase-related kinase family)

M.W. – Molecular weight

ng - Nanograms

PCR - Polymerase chain reaction

PD - PD0325901 is an orally active, selective and non-ATP-competitive MEK inhibitor

Pen/Strep - Penicillin and Streptomycin

PFA- Paraformaldehyde

pg - Picograms

PGCs – Primordial germ cells

PGCLCs - primordial germ cell-like cells

PI - Propidium iodide

PS807/11-Rb - phosphorylated Serine807/11-Rb

PS780-Rb - phosphorylated Serine780-Rb

Rb - Retinoblastoma protein, its phosphorylated form – P-Rb

RCF - Relative centrifugal force

Rpm - Revolutions per minute

RT - Room temperature

SDS - Sodium dodecyl sulfate

sec - Seconds

sgDNA – Single guide deoxyribonucleic acid

TBS - Tris-buffered saline

TBST - 1X TBS with 0.1 µL/mL Triton™ X-100

U – International unit of enzyme's catalytic activity

X-Gal - 5-bromo-4-chloro-3-indolyl-β-D-galactopyranoside, inert chromogenic substrate for beta-galactosidase

1. Introduction

1.1. Mammalian embryonic development

Mammalian embryonic development occurs according to a regulative schedule at molecular, cellular, tissue and organismal levels, initiating at fertilization and ending with the organism's birth[1]. Through these processes, cells can divide and differentiate to give rise to different tissues, with the range of differentiation options open to a cell described as its potency. The embryonic development cycle begins when the zygote is formed, after fusion of sperm and egg cells called fertilization (E0.5). The zygote starts undergoes cleavage divisions to give rise to two cells (E1.5), called blastomeres, that will continue to divide and form the morula at the 16-cell/blastomeres stage (E2.5)[1]. Early in mammalian embryonic development, the zygote and early blastomeres are totipotent, meaning these single cells can give rise to extra-embryonic and embryonic structures thus, to an entire functional organism.

1.1.1. Pluripotency

Pluripotency is characterized by the capacity of a single cell to form all cell types from each of the three primary cell layers – endoderm (inner layer), mesoderm (middle layer) and ectoderm (outer layer) (**Fig.1.1**) – as well as germ cells. Pluripotency is largely controlled and maintained by the core transcription factors Oct4, Nanog and Sox2 and cells from the pluripotent state can also be identified by the present of the alkaline phosphatase enzyme[2–5]. Pluripotent cells arise in the pre-implantation epiblast (EPI) at the blastocyst stage (Mouse E4.5 and Human E7 stages) and persist until the epiblast's gastrula stage, by which time commitment to different cell lineages has occurred (E8.0) (**Fig.1.1**)[6]. Therefore, pluripotency is transient and various studies have described its different stages.

Naïve pluripotency (E4.5-E5.0) is the earliest stage of pluripotency, and is found in the cells of the EPI[7,8]. Naïve cells have the capacity to form both somatic and germ lines and this property can be captured *in vitro* in embryonic stem cells (ESCs). In addition, ESCs can form high contribution chimaeras – the term used for a mixture of host and donor cells -, and also exhibit germline transmission[9]. The contribution to chimaeras proves that the injected cells maintain their capacity to continue embryonic development without development defects.

After implantation, mouse epiblast cells enter a formative state (E5.5-E6). Formative stem cells (FSCs) have the capacity to form the three germ cell layers and have direct responsiveness to form primordial germ cells (PGCs) but lose the competency to form naïve stem cells. Loss of competency may be due to downregulation of $KLF4^+$ - a naïve cell transcription factor – present in these cells. In 2021, FSCs were inject into blastocysts and contributed to chimaeras[10]. FSCs' contribution to chimaeras was less efficient than ESCs. Also, *in vitro*, formative cells can be captured for many passages without FGF (fibroblast growth factor), and if cultured with FGF, FSCs progress forward to make primed epiblast stem cells (EpiSCs)[11].

Although formative pluripotency has been studied as a different stage, *in vivo*, it is a transient stage between naïve and primed pluripotency states. Primed pluripotency, found at the late-gastrulation anterior primitive streak (E6/6.5), is the latest pluripotency state[12]. With the capacity to form the three germ line layers and unable to give rise to PGCs *in vivo*[13], EpiSCs do not readily reform naïve or formative pluripotent stem cells. *In vitro*, EpiSCs can be maintained by FGF and Activin supplemented medium, and Wnt inhibitor is used to obtain homogenic cell culture[10,14], and only contribute for chimeras, after blastocyst injection, if genetically manipulated to one of the earlier pluripotency stages[15].

Additionally, in 2006, the reprogramming of pluripotent stem cells (iPSCs) from differentiated cells with the Yamanaka factors or OSKM (Oct4, Sox2, Klf4 and c-Myc), was reported by Takahashi and Yamanaka[16]. This study goes towards generating pluripotent cells for clinical treatments and to improve our understanding of both disease and development. iPSCs are similar to ESCs and, with specific medium, can be differentiated to any required cell layer.

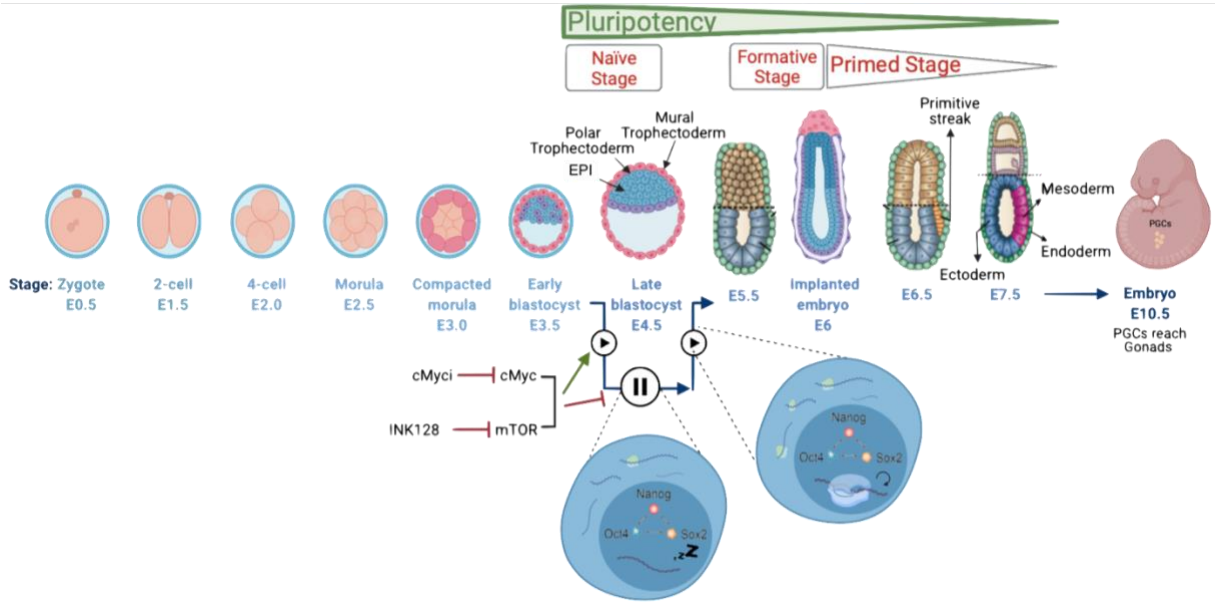

Figure 1-1. ***Mouse embryonic developmental representative scheme****. Representation of mouse embryonic development from 0.5 to 10.5 days, with pluripotent capacity between E4.5 and E8 stages. ICM cells can be isolated and maintained in vitro, in 2i/LIF medium, being defined as ESCs. A diapause-like stage can be induced, in vitro, in these mESCs with a mTOR inhibitor supplementation, which is represented with the paused bottom. c-Myc inhibition may also be used to induce diapause in mESCs however, with lower efficiency, since it can only be maintained for one day.*

1.1.2. Mouse embryonic stem cells

In 1959, Leroy Stevens, when studying teratocarcinomas' properties, in mouse strain 129, excised cells from these teratoma tumour growths, transplanted them into other mice and found that they gave rise to cells that resembled early developmental tissues[17]. A few years later, in 1970, Stevens found that PGCs were competent to form teratomas but also embryonic carcinomas (ECs) - cells that resemble the early developmental niche - leading the way to the generation of stem cells[18]. These embryonic like cells were then shown to contribute to chimeras when injected in blastocysts, indicating their capacity to reintegrate into a developing organism and demonstrating their pluripotency[19]. However, contribution was only at a low level, and upon mating chimaeras, germline transmission was not reproducibly obtained due to genetic abnormalities present in these tumour-derived cells. After these landmarks, mESCs were then derived from embryos and cultured *in vitro* on mouse embryonic feeders (MEFs) for several passages and mESC pluripotency was confirmed with chimeric contribution and germline transmission[20,21].

In vitro, mESCs were first isolated from the EPI of the blastocyst[20–22]. The capacity of cells to continuously self-renew, i.e., to proliferate while maintaining developmental potency, is possible in appropriate culture conditions, which for mESCs typically contain the growth factor called leukaemia inhibitor factor (LIF)[23]. However, in 2008, it was reported that ESCs are morphologically heterogeneous. One hypothesis is that this is due to a metastable state that shifts between ICM and later epiblast stages[24]. In cultures, this unstable state and heterogeneity could lead to inappropriate differentiation *in vitro*[25]. This led to the development of conditions that can maintain ES cells in more

homogenous cultures. It was found that the co-inhibition (2i) of MEK, blocking ERK1/2 signalling pathway, and glycogen synthase kinase 3 – by PD0325901 (Mirdametinib) and CHIR99021 respectively – promotes morphological and molecular homogeneity in ESCs obtained in *in vitro* cultures in 2i/LIF medium, and also that, cells in 2i medium have a transcriptome similar to EPI[26,27].

1.2. Diapause

In over 130 mammalian species it has been reported that, during development, the embryo can undergo an embryonic dormancy stage called diapause. Diapause is a natural, conserved phenomenon, thought to further the mother's and offspring's chances of survival, by coordinating the process of development with favourable environmental conditions[28] such as seasonal supplies of food, temperature, photoperiod and lactation[29]. Diapause maintenance and termination are maternally controlled[30]. Moreover, some mammalian embryos can fail development due to genetic aberrations. In these cases, pausing at blastocyst stage has been suggested to improve development for only successful embryos[31].

In mice, development stays on hold when the embryonic blastocyst does not immediately implant in the uterus, normally occurring when pregnant females are lactating, and so induced by lactation's stimulation[32]. Also, this can be artificially induced by injection of oestrogen antagonists or by surgical removal of ovaries (ovariectomy) at embryonic day E3.5, both of which prevent the ovarian oestradiol surge, necessary for implantation[33]. In both cases, diapause can be maintained by daily administration of progesterone[34].

In mouse, diapause may persist *in vivo* for twice as long as gestation and *in vitro,* for up to 36 days[35]. Diapause exit is marked once lactation terminates, although depending on the length of diapause, on average within 12h of the oestrogen surge, which increases uterine receptivity, or experimentally by injection of oestradiol[36].

In vitro, a similar paused state can be mimicked by the inhibition of c-Myc (**Fig.1.1**) in mouse ES cells, which induces reversible dormancy[37]. In 2016, it was reported that mTOR inhibition (**Fig.1.1**), in *ex vivo* blastocysts and in mESCs, has the same effect in development and seems to prolong the paused state between 9-12 days, instead of only one day[38]. Moreover, overexpression of microRNA let-7 was also shown to induce diapause-like paused state *in vitro,* up to 14 days[39]. Despite the different methods, all three induced states can be released from paused and transferred to pseudo-pregnant female mice.

Diapause has been identified as a stage with low or no proliferation rate hence some studies have tried to characterize growth during this process, and in 2019 was reported that mouse embryo's (obtained by ovariectomy and injected daily with progesterone) regions reach dormancy at different times. Within one day of diapause induction, it was shown that mural trophectoderm stops proliferating while polar trophectoderm and ICM reduces its proliferation rate up to day five after diapause induction, showing no proliferation after that time[36,40]. Despite the variability of cell proliferation between mouse embryos intra- and inter-strains, it was reported that mouse embryo grows ~ 140 cells during diapause and suggested that almost all the embryo cells are in G0 phase of cell cycle, after five days of diapause induction[36], in accordance with the results showing that ICM cells are metabolically quiescent[40]. But, whether mESCs induced into a paused stage using different methods represent a similar cell state remains controversial and thus requires further study.

In humans, it was reported previously that diapause may occur[41] but, it still is a poorly understood phenomenon due to practical and ethical considerations. However, in other animals delayed

implantation appears to enhance the development potential of the embryo[42–45]. These findings could be caused by cellular repair while being in the development arrest, and if applied in humans, embryonic diapause can be used to prolong and/or enhance embryos culture conditions for assisted reproduction technologies, such as *in vitro* fertilisation (IVF). Also, if embryonic diapause is confirmed in humans, some diagnostics should be revised, such as "intra uterine growth restriction (IUGR)" or "prolonged gestation", and the use of last menstrual period's day to estimate the pregnancy duration may will be misleading. In these cases, understanding diapause regulation is crucial to get a more precise implantation date and so the following gestation duration. This would help to reduce the uncertainty of overdue dates and to prevent unnecessary surgical interventions.

Additionally, it's reported that some cancers' cells resist to anti-cancer treatment. After successful treatment of the primary tumour, these cells can reactivate and cause disease relapse. This drug resistance is suggested to be acquired by undergoing a dormancy state. Even more intriguing is that in some cases resistant cells can stay dormant for years. Recent studies have been identifying this dormancy as a diapause-like state. Besides our knowledge on this field, the regulation behind the resistant stage of tumour cells is still poorly understood, complicating cancer treatment. Therefore, diapause studies may improve our knowledge in both the developmental biology and cancer fields.

1.3. Cell Cycle

1.3.1. Cell Cycle Arrest

The cell cycle is the process through which each cell divides to give two daughter cells, and in eukaryotes it is divided into 4 stages: G1 (Gap 1), S (DNA replication – synthesis phase), G2 (Gap 2) and M (Mitosis). Those phases are regulated by a Cyclins (Cycs) and Cyclin-dependent kinases (CDKs) complexes, their negative regulators, the Cyclin-dependent kinase inhibitors (CDKIs) (**Fig. 1.2A**) and positive regulators - for e.g., cell division cycle 25 protein (cdc25) or CDK-activating kinase (CAK). When a cell grows and begins the cell cycle, G1 phase starts and the cell has increased levels of Cyclin D. At this time, CycD binds to CDK4/6 forms CycD-CDK4/6 complex and initiates retinoblastoma protein (Rb) phosphorylation, which becomes hyperphosphorylated (P-Rb) later in G1[46]. However, while Rb protein is hypophosphorylated, Rb protein binds and inhibits E2F and E2F target genes are repressed. When Rb becomes hyperphosphorylated, E2F is activated and so are its target genes. E2F target genes are required for G1/S phase transition, including Cyclin E (CycE). CycE forms a complex with CDK2 having positive feedback on Rb protein phosphorylation, and this feedback leads to Rb hyperphosphorylation, E2F activation and drives cells from G1 into S phase[47] (**Fig. 1.2B**).

At the beginning of S phase, CycE-CDK2 complex is replaced by Cyclin A-CDK2 complex[48]. Along this process, CDKIs help ensuring presence of the right Cyc-CDK complex for each phase, preventing backwards progression, and CDKIs also stop cell cycle in critical situations, such as DNA damage. CDKIs are divided in two families of proteins, INK4 and CIP/KIP. The CIP/KIP family is made up to three proteins (p21, p27 and p57) that bind to both cyclin and CDK. Cell cycle regulators as p27 and p21 are present through the whole cell cycle and bind to Cyclin D, E and A-dependent kinase complexes[49]. p27 is abundant in quiescence[49]. Moreover, as well as inhibiting CycE/CDK2 complexes, p27 is also inhibited by CycE/CDK2-dependent phosphorylation during G1/S phase transition[50,51], generating a double negative feedback loop. Additionally, is reported that p21 and p27 bind and promote activation of CycD-CDK4/6 complexes by localization the complex into the nucleus and by binding to CycD and increasing its stability. On the other hand, this CycD-CDK4/6-Cip/Kip complexes prevent Cip/Kip-CDK2 binding maintaining CDK2 activity. Moreover, p53-dependent activation of p21,

inhibits CycE/CDK2 complex, downstream of DNA damage, arresting the cell cycle in G1/S transition, inhibiting Rb phosphorylation [52].

Outside the proliferative phases of the cell cycle (G1, S, G2, M), cells can enter prolonged cell cycle arrest – for example quiescence or senescence. Quiescence is a hypotrophic and reversible state, also called G0 phase that occurs in G1, prior to the to the restriction point or in G2. By contrast, senescence is irreversible, and a hypertrophic cell cycle exit, that can also take place either in G1 or G2. In 2016, a review regarding these differences reported that quiescence occurs due to lack of nutrition and growth factors whereas senescence takes place due to aging, serious DNA damage and other mutagens. Furthermore, Barr and colleagues, saw that naturally occurring DNA damage in S-phase causes p53-dependent accumulation of p21 during mother G2- and daughter G1-phases. This suggests that accumulation of p21 serves to integrate information on DNA damage for the proliferation-quiescence decision in G1[53].

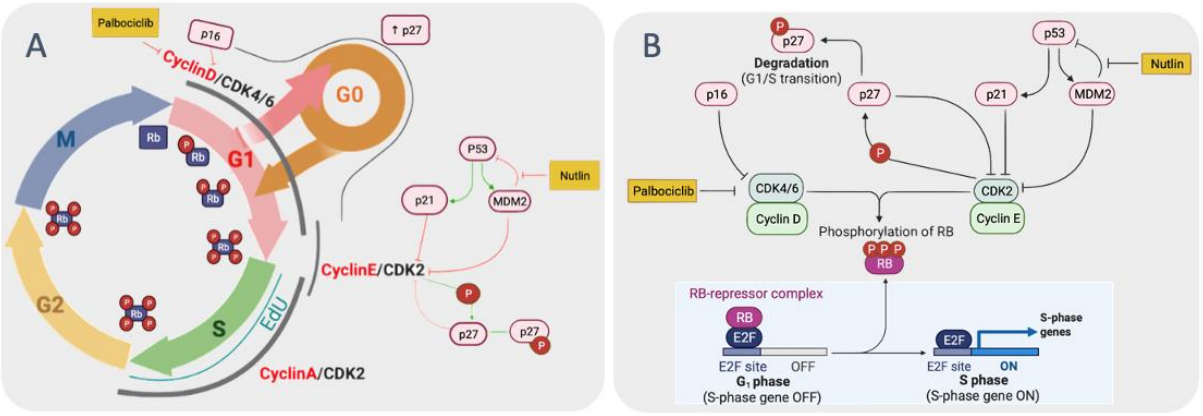

Figure 1-2. ***Cell Cycle regulation schemes. A and B-*** *The cell cycle is regulated by Cyclins-CDKs complexes and by negative/positive regulators of these complexes. CycD-CDK4/6 is the complex regulating G1-phase progression, specially by phosphorylating Rb protein. The non-phosphorylated form of Rb protein is bonded to E2F factor, inhibiting its activity and maintaining the S-phase genes' expression off. When Rb is phosphorylated, releases E2F, which will initiate the S-phase genes transcription. Within these genes for S-phase, CycE is expressed to induce G1-phase to S-phase transition. Additionally, CycE in complex with CDK2 also cooperate into a feedback loop to phosphorylate Rb protein, promoting faster S-phase entrance. Moreover, CycA-CDK2 complex take place to regulate the cycle while entering and throughout the S-phase. Scheme B is adapted from* ***The Molecular Biology of Cancer****, 2nd ed., 2013, Wiley.*

1.3.2. Mouse ESCs Cell Cycle

mESCs have a high rate of proliferation, doubling in ~12-14h[54], and have a characteristic cell cycle with a short G1 phase compared with somatic cells (**Fig. 1.3**). In serum cultured mouse pluripotent stem cells (mPSCs), this reduced G1 phase is due to the lack of MAPK, CycD/CDK and P-Rb control[55]. It has been reported that mESCs cultured in 2i+LIF medium show a slightly longer G1 phase, with hypo-phosphorylated Rb and a shorter G2 phase, comparing to serum mPSCs, implying that they have a G1 restriction point[56]. mESCs cells also show high levels of Cyclin E and A and of CDK1/2 activities throughout the cell cycle[57,58], in contrast with the phase-specific expression of Cyclin E and A in somatic cells' cell cycle. These findings are supported by coupled regulations between some cell cycle regulators and pluripotency factors, for example, low expression of FBXW7 and miR-15a permits upregulation of Cyclin E, which is also positively controlled by binding sites on its gene (*CcneI*) for pluripotency factors, as ESRRB, KLF4 and TFCP2l1[59].

Additionally, constitutive degradation of CDKIs likely contributes to the observed higher activity of CDKs in pluripotent cells. For instance, in 2010, it was reported that in human ESCs overexpression of SKP2 leads to the degradation of $p27^{KIP1}$ [60]. This would allow CDK2 to be active and

it may in turn phosphorylate and stabilize OCT4, SOX2 and NANOG, thus promoting rapid G1/S phase transition while maintaining the developmental pluripotency of mESCs as described in previous studies[61,62].

On the other hand, even though it has been described that the cell cycle regulator p53 can repress Nanog transcription, its expression is stabilized in higher levels than somatic cells and more localized in the cytoplasm[63,64]. Since p53 regulates positively p21, higher levels of p21 might be expected in mESCs. However, it has been shown that p21 expression is negatively stabilized at chromatin level and by rapid proteasome-mediated degradation[65,66]. Low levels of p21 might explain the lack of G1 control in mESCs. Consequently, in studies where p21 levels accumulate and the proportion of G1-phase cells increase, downregulation of pluripotent genes as *Oct4* and *Nanog* occurs, suggesting that increase of p21 levels leads to differentiation in mESCs[65].

Therefore, whether the lack of G1 control in naïve mESCs is due to hyperphosphorylation of Rb or high degradation of p21 is still unclear and so further studies are required to answer this question. In addition, it remains unclear if mESCs can go through G1-phase arrest and if this event is p21-dependent or if other mechanisms are involved in this process.

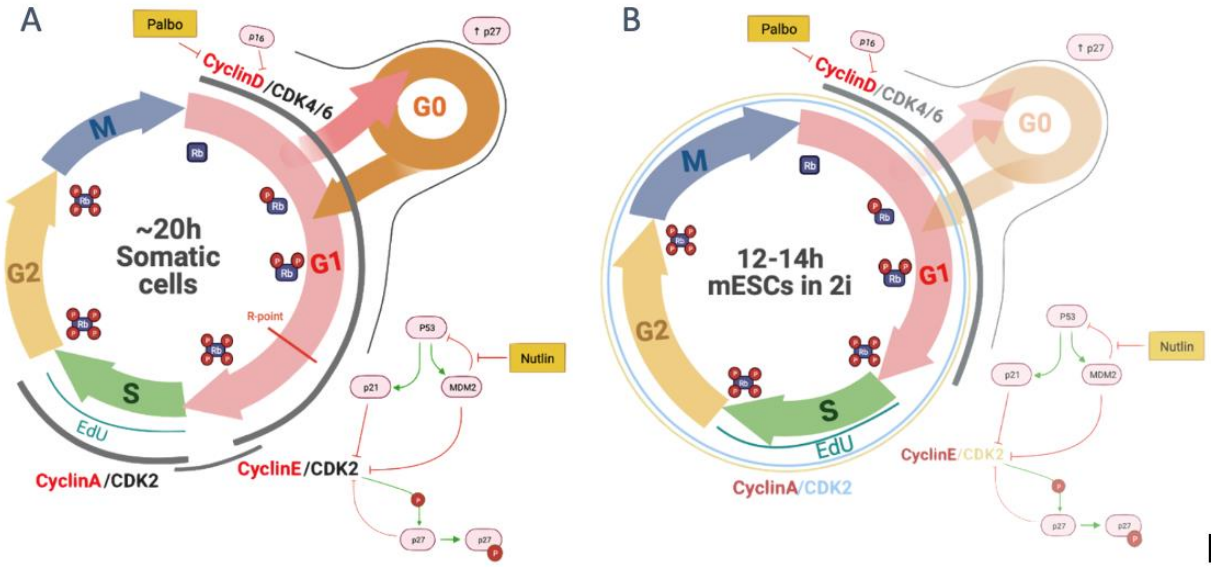

Figure 1-3. ***Cell Cycle control in somatic cells and in mouse naïve pluripotent stem cells.*** *Cell cycle is divided into 4 phases: G1-, S-, G2- and Mitotic-phase.* ***A****- In somatic cells, an average cell cycle lasts for ~20h with the expression of different Cyclin-CDK complexes specific for each phase. In these cells CycD-CDK4/6 complex is expressed during G1-phase, phosphorylates Rb protein and activates CycE-CDK2 complex expression (****Fig.1.2.B****). CycE-CDK2 promotes S-phase entrance, where CycA-CDK2 complex upregulation takes place, and regulates this phase until progression into G2-phase.* ***B****- Naïve mESCs have rapid cell division mainly due to shorter G1-phase that reflects on a ~12-14h cell cycle. In mESCs' cell cycle, CycE and A have elevated levels through the cycle, high levels of CycD-CDK4/6 complex (specifically for G1-phase) that permits their hyperphosphorylation of Rb leading to fast entrance into S-phase.*

1.4. Project's Objectives

Although it is known how diapause is induced *in vivo* and how to induce it *in vitro*, its regulation mechanisms are still unclear. For example, while it is known that p21 increases and mediates G0/G1 phase cell retainment and DNA replication reduction when blastocyst are induced to diapause, further studies are needed to understand this mechanism when the diapause-like state is induced in mESCs. In mESCs paused with c-Myc inhibitor, it has been shown that cells are prevented from going through S-phase, suggesting an arrest in G0/1 or in G2 phases. In contrast, when mTOR inhibitor is used, cells are distributed along cell cycle phases similarly to non-arrested cells but with low proliferation rate. These

results suggest differences between regulation of diapause *in vivo* and *in vitro, a*nd between different *in vitro* systems. Therefore, further studies are required to understand if during diapause cells are completely in paused state or cells' progression is slowed down and how this process is regulated, especially at the cell cycle level.

My aim is to understand how the cell cycle is regulated in ESCs as cells enter and exit diapause. To analyse this process, I investigated the cell cycle from induced diapause cells, *in vitro,* by testing and comparing cell cycle inhibitors. I analysed the regulation of cell cycle proteins known to be linked with entry into and exit from quiescent states, using quantitative single-cell imaging. I also aim to develop a system to be able to follow diapause entry and exit in real-time. For this, CRISPR/Cas9 is used to engineer a fluorescent reporter of a cell cycle regulator. This cell reporter can then be screened using quantitative live imaging, while ESCs enter and exit the paused state. Together these evaluations, inform our understanding of how mouse embryos can enter this unique cell state.

Regarding the cell cycle, DNA damage checkpoints have a high importance by the fact that their dysregulation is one of the fundamental bases of oncogenesis. So, understanding those mechanisms may drive us to significant novel cancer therapy approaches. On the other hand, it has been reported that some cancer cells can tolerate some chemical therapies by entering into a similar to diapause stage[67]. The research about diapause-like stage in cancer cells can bring crucial knowledge to find combinations of treatments to target those issues.

2. Methods

2.1. Mouse ES cell culture

E14 mouse embryonic stem cell (E14Tg2A, Hooper, M. et al. 1987[68]) were cultured in 48,6% Dulbecco's Modified Eagle's Medium/F-12 (DMEM/F12, **Gibco**, #21331020), 48,6% Neurobasal medium (**Gibco**, #21103049), 1% B-27 supplement (**Gibco**, #17504-044), 0.5% N-2 supplement (**Gibco**, #17502-048), 1% L-Glutamine (**Gibco**, #25030-024), 0.2% β-mercaptoethanol (**Gibco**) and with 100 U of Leukaemia Inhibitor Factor, 1 µM PD0325901 (**Caltag Med System**) and 3 µM CHIR99021 (**Cambridge Bioscience**) as feeders, in the incubator humidified at 7% CO_2 and 37 °C. Tissue culture plates and flasks (T12.5 and T25, **FALCON**) were used for adherent routine cultures coated with 0.1% Gelatine (**Sigma-Aldrich**, #G1393-20) in PBS. Cultures were monitored daily and split every 2-3 days using Accutase (**Merk Millipore**, #SF006) to form single cell suspension and washed in DMEM/F12 (**Sigma Aldrich**, #D6421-500) with 1% BSA.

2.2. Colony forming assay

Colony formation assays were done with 6-well plate (**Nunc FALCON**), coated with laminin (**Sigma Aldrich**, #L2020-1), overnight in the incubator at 37 °C. Laminin was aspirated and 1 mL of 2i/LIF medium added into each well, which were left at 37 °C. Cells were prepared in a suspension to seed 200 cells, with 1.5 mL, dispersed in each well, in a total volume of 2,5 mL and placed in the incubator humidified at 7% CO_2 and 37 °C. Cells were treated with 0.2 µM mTORi (INK-128, **Selleckchem**, #S2811), 10 µM Palbociclib, 10 µM Nutlin (**Sigma**) or 1:100 DMSO (**Sigma**) after one day of growing, without medium replacement. After 4-5 days, colonies were rinsed with PBS and fixed with 4% of paraformaldehyde (PFA, **Thermofisher**, #28908). To image pluripotent colonies, cells were stained with alkaline phosphatase, according to manufacturer's instruction (**Sigma Aldrich**). Wells were stained with 1 mL of alkaline-dye mixture for 15 minutes, at 18-26 °C in the dark, washed for two

minutes with deionized water, and then washed and air dried. Whole wells images were taken with Leica M80 zoom stereomicrospe and then counted with Fiji software.

2.3. Quantitative mESCs immunocytochemistry imaging

2.3.1. mESCs immunocytochemistry

Immunocytochemistry assays were done in 96 well CellCarrierUltra Microplate (**PerkinElmer**), coated with 50 µL 1:1 of 1-2 µg/mL Laminin:0.1% Gelatine for one hour, in the incubator (37 °C) which was removed before seeding cells. Cells were seeded at 1.8 x 10^4 cells/cm^2 density, in 2i/LIF medium and with 50 µl of final volume per well. For the different conditions, 50 µL of inhibitor treatments were added 24h after seeding, by without replacing the medium with inhibitors diluted in 2i/LIF medium – 10 µM Nutlin (**Sigma**), 10 µM Palbociclib, 0.2 µM mTORi (INK-128, **Selleckchem**) – and incubated for 24-48h before fixing cells. Also, a negative control was performed with 1:100 DMSO (**Sigma**) and for untreated cells only 2i/LIF medium was added. For DNA synthesis staining, EdU incorporation assay was performed by adding 10 µM EdU (**Invitrogen**, #C10340), without replacing the medium, 20 minutes before fixing cells. For Palbociclib and DMSO dose curves, cells were treated with five different concentrations (10µM, 5 µM, 2.5 µM 1.25 µM, 0.625 µM and 1:16000, 1:800, 1:400, 1:200, 1:100 respectively) for 24h or 48h hours.

Before staining, cells were fixed with 150 µL of 8% PFA (**Thermofisher**, #28908), without taking the culture's medium (150 µL) for 4% of final concentration, in clean and filtered phosphate buffered saline (PBS) for 15 minutes, washed three times with PBS, permeabilized with 0.5% Triton X-100 in PBS for 15 minutes, washed three times with PBS, blocked (except the EdU treated cells) for 30 minutes with 2% Bovine serum albumin (BSA, **Fisher Bioreagents**, #BP9701-100) in PBS. Cells treated with EdU were washed with PBS, 50 µL of EdU additive solution (see **table 2.1**) was added in each well, incubated for 30 minutes in the dark at room temperature and blocked for 30 minutes with 2% BSA in PBS. Then, cells were washed three times with PBS and incubated overnight at 4 °C with primary antibodies (see **table 2.1**) in blocking solution after a spin down in centrifuge for one minute at 800 rpm, room temperature. Cells were washed in PBS, incubated with 2 µg/mL fluorescence-conjugated secondary antibodies goat anti-mouse 488 (green) and goat anti-rabbit 568 (red) (**Invitrogen**, #A-10680 and #A-11011 respectively) in the dark, at room temperature. After one hour, cells were washed three times in PBS, stained with Hoechst (**EnzoLifeScience, #**ENZ-52401) at 1 µg/mL in PBS and incubated at room temperature, in the dark for 15 minutes. Finalizing this process, the wells were washed in PBS, left with 50 µL of PBS and the plate sealed with foil seal. The plate was stored in the fridge (4 °C) if not immediately imaged and after imaging.

Table 2.1 – Immunostaining assay solutions recipes.

Solutions		Company	Catalogue number	Final Concentration	Final volume
1º Anti-Bs (in Blocking solution)	Rabbit Anti PhosphoS807/11 Rb	Cell Signaling Technology	8516S	0.05 µg/mL	-
	Rabbit Anti PhosphoS780	Cell Signaling Technology	8180S	0.1 µg/mL	-

	Mouse Anti Rb	Cell Signaling Technology	9309S	0.1µg/mL	-
	Rabbit Anti Cyclin D1	Cell Signaling Technology	2978S	0.4 µg/mL	-
EdU Additive solution	Sterile water	-	-	-	870 µL
	1M Tris pH7.5	-	-	0.1 M	100 µL
	CuSO4	Invitrogen	C10340	4 mM	10 µL
	Alexa Fluor 647 dye	Invitrogen	C10340	5 µM	10 µL
	Ascorbate	Invitrogen	C10340	10 mM	10 µL

2.3.2. Imaging and quantitative analysis

Imaging was performed using the Operetta CLS High-Content Analysis microscope. Images were captured in one z-stack layer and with the respective LEDs to obtain the different channels of staining - 461nm channel for Hoechst staining, 488nm and 568nm for the antibodies staining and 647nm for EdU. After this, the Harmony 4.5 software was used for image quantification. Measurement of nuclear intensities of proteins was performed as following (**Fig. 2.1)**: Nuclei were segmented based on Hoechst intensity and with ~20 µm^2 of area. Nuclei at the edge of the image were excluded. To decrease errors of intensity measures due to overlap of neighbour-cell's intensity, cell region was select for 55% inner nuclei. The fluorescence intensity of individual proteins, Hoechst and EdU was then calculated in each selected cell region. After EdU intensity calculation, EdU positive cells were selected as a new population by a defined threshold (that was defined individually for each experiment based on EdU staining intensity and imaging conditions). The list of outputs for each selected population was defined and these quantitative results were exported and then analysed and plotted with mathematical software - Excel and Prism (GraphPad software).

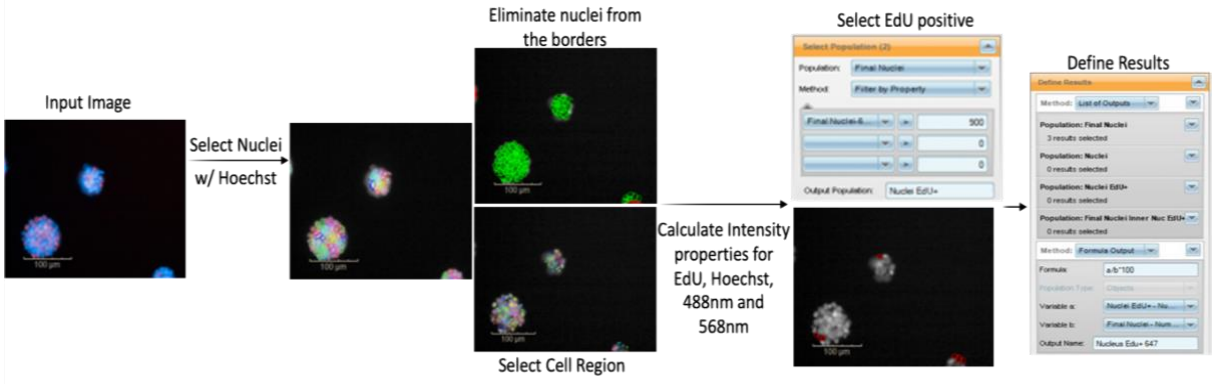

Figure 2-1. ***Image analyses scheme****. Images were captured using the Operetta CLS HC Analysis microscope and analysed by Harmony 4.5 software. For image analysis, nuclei were segmented on Hoechst intensity, and a population of nuclei was selected by eliminating edges nuclei. In each nucleus, a smaller cell region was selected and intensities of Hoechst, EdU and individual proteins were calculated from each selected cell region. EdU positive intensity threshold was defined. Based on that threshold, the population of positive cells was selected. After this, list of outputs was defined, and results were exported.*

2.4. Cell cycle analysis by flow cytometry

To consolidate some results from the immunocytochemistry imaging assay and confirm in which phase of cell cycle the treated cells might be, a cell cycle analysis assay was performed. Cells were plated in 6-well plates and seeded at 1.5 x 10^4cells/cm^2 density, in 2i/LIF medium and with 1 mL of final volume per well. For the different conditions, 500 µL of 2i/LIF medium with inhibitors – 10 µM Nutlin (**Sigma**), 10 µM Palbociclib, 0.2 µM mTORi (INK-128, **Selleckchem**) –, negative control (1:100 DMSO, **Sigma**) diluted or untreated were added 24h after seeding. This 500 µL were added to culture without replacing the medium and treated cultures were incubated for 24h and 48h before fixing cells.

Based on reading the EdU incorporation (if cells went through S phase) and propidium iodide (PI, which binds and stains DNA) fluorescence with a flow cytometry analyser, is possible to evaluate the percentage of cells that are going through each cell cycle phase. Therefore, cells were pulsed with 100 µM EdU for 45min. and harvested with accutase. Using Click-iT EdU Flow Cytometry Assay Kit (**Thermofisher**, #C10424) according to the manufacturer's instructions, cells were fixed, permeabilized and EdU was detected by Click-iT Alexa Fluor 647. Each cells sample was washed and suspended in PBS with 0.1 TritonX-100, 20 µg/mL PI solution and 200 µg/mL RNAseA and incubated for 30min. in the dark. After staining, samples were analysed by Analyser LSR II instrument and following results were plotted and analysed by FlowJo software. Cells were quantified as being in G1- and G2-phase if their EdU intensity was below a threshold level defined by the highest EdU intensity level of a cell from the negative control sample. This negative control had EdU pulsed and PI staining but was not stained for EdU. In opposite, cells were quantified as being in S-phase if their EdU intensity was above this same threshold level. On the other hand, G1-phase gate was selected as being below a threshold level decided by PI intensity distribution, and G2-phase gates as being above the same threshold. Moreover, it was important to consider that the PI intensity values from the G2-phase cells are around the double of PI intensity values from the G1-phase cells.

2.5. E14 engineering with CRIPR/Cas9 for p21 tagging with mRuby

2.5.1. Polymerase Chain Reaction (PCR) and genomic DNA extraction

Cas9 with gRNA has the capacity to recognise and cut a specific target region in the genome. However, this cassette will form double strand breaks (DSB) in the DNA but doesn't repair them. These DSBs will be repaired by a homology recombination in two regions between the genome and a given DNA molecule called left and right homology arms (LHA and RHA, respectively). For this the given DNA (gDNA) molecule will contain the homology arms and the sequence we want to incorporate in the genome within them – mRuby DNA sequence.

For this, mRuby cDNA was amplified from a plasmid by PCR (**Fig. 2.2.A**) in a 50 µL reaction containing 2 ng template DNA, 2 U Q5 High-Fidelity DNA polymerase (**BioLabs**), 0.5 µM each primer (**Table 2.2**), 0.2 mM dNTPs, 1x Q5 Buffer (**BioLabs**). The cycling protocol was performed as following, with step 2 repeated for 25 cycles:

98°C 30 sec

98°C 5 sec, 55°C 10 sec, 72°C 60 sec

72°C 120 sec

4°C, Hold

To isolate the amplified fragment, the 50 µL reaction product with 1x Gel Loading Dye Purple (**BioLAbs**, #B7024S) was segregated by size via 1% (w/v) agarose (**Sigma Aldrich**, #A9539-200) gel electrophoresis containing 1x SyBR Safe DNA Stain (**Invitrogen**, S33102). For fragments size visualization, 10 µL 1kb DNA Ladder (**BioLAbs**, #N3232L) was used. Electrophoresis was carried out in 1x TBE buffer and run at 110V for 30 min, then DNA fragments were excised and purified using the QIAquick PCR Gel Extraction Kit and eluted in 30 µL H_2O, ready for the required plasmid construction.

2.5.2. Gibson Assembly, Transformation - Plasmid construction and Amplification

To introduce the repair template in the cells, a plasmid with mRuby DNA and both homology arms, was constructed by Gibson Assembly (**Fig. 2.2.B**) using the NEB Quick Ligation Kit, according to manufacturer's guidelines. 363 ng linearized pSKII(-) with EcoRV, 67 ng LHR, 66 ng RHA and 42 ng mRuby extracted DNA were incubated with 10 µL NEB Builder for one hour at 50 °C. 50 µL 5-alpha Competent E. coli cells (**NEB**, C2987I) were transformed with 2 µL of assembly reaction product, according to manufacturer's high efficiency transformation protocol, with incubation overnight at 37 °C in presence of X-Gal, for positive colonies selection, i.e., colonies containing the relevant transformation. Single positive colonies were piked and inoculated in 3 mL cultures of LB-broth containing 100 µg/mL Ampicillin and incubated at 37 °C and 220 rpm, overnight. To confirm if the picked colonies had and well-constructed the plasmid, the next day, 2.5 mL bacteria were pelleted at 4500 x g, for 10 min., and DNA extracted and purified by QIAprep Spin Miniprep Kit, according to manufacturer's guidelines. Purified DNA, containing the required plasmid, was eluted in 30 µL of H_2O, stored at – 20 °C, and sequenced for T7/T3 primers and inner mRuby Forward/Reverse primers. 0.5 mL bacteria were stored at 4 °C and posteriorly used for high-scale, high quality plasmid DNA amplification. For this, bacteria were incubated in 250 mL LB-broth containing 100 µg/mL Ampicillin and incubated at 37 °C and 220 rpm, overnight. Cultures were centrifuged at 4500 x g for 15 min. and the DNA extracted using HiSpeed Plasmid Maxi Kit and eluted in 0.5 mL of H_2O. Before transfection experiments, the concentration of plasmid DNA was determined according to A_{260} readings using a NanoDrop spectrophotometer and sequenced as before.

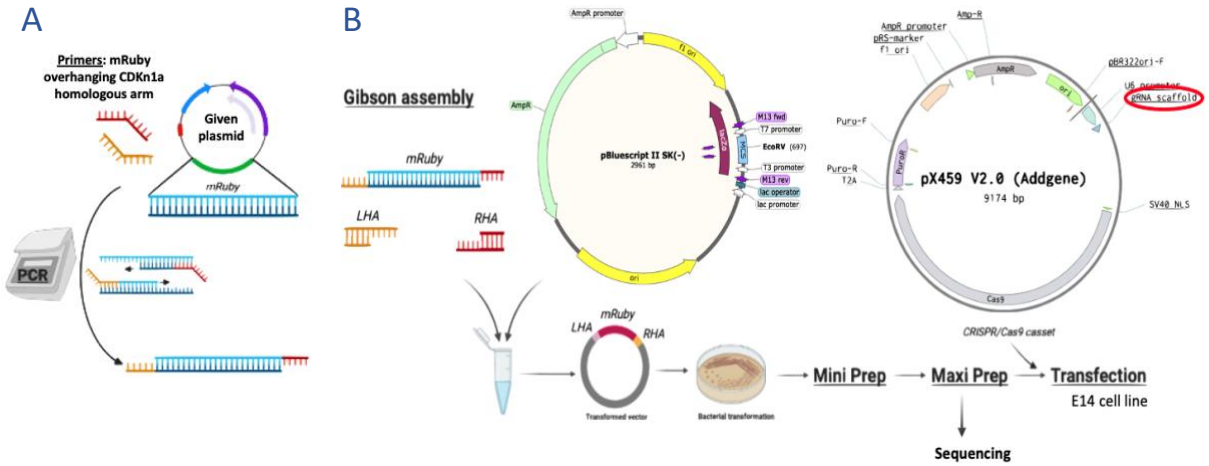

Figure 2-2 ***Plasmid construction for recombinant template and amplification scheme****.* ***A****- Polymerase Chain Reaction (PCR): mRuby DNA was extracted from an existed plasmid by PCR with the mRuby overhanging Cdkn1a homologous arm primers (***Table 2.2****). The primers were design to obtain a product with sticky ends that complement with the homology arms that will be used for recombination during transfection.* ***B****- Gibson Assembly and Transformation: Gibson Assembly was performed to join mRuby DNA and right and left homology arms into a pBluescriptIISK(-) plasmid. This plasmid would be a donor of the repair template for recombination during transfection thus, it was required to be amplified. The amplification of the plasmid was performed by transforming into bacteria. Bacteria were incubated overnight for small (Mini prep) and then large (Maxi prep) cultures. DNA from these bacteria' cultures was purified and sequenced to confirm if the constructed was successfully*

obtained. After having the constructed plasmid, the E14 cell line was transfected with this plasmid together with a CRISPR/Cas9 cassette plasmid.

2.5.3. CRISPR-Cas9 Transfection

CRISPR gRNA for mouse p21 gene was already incorporated in a PX459 V2.0 plasmid (**Addgene plasmid**, #62988) with mCherry. ~300.000 E14Tg2A cells were plated, in 6-well plates (**Nunc FALCON**) coated with Laminin, with 1.6 mL CH/LIF medium (CL medium) + 400 µL of transfection reaction and placed in the incubator humidified at 7% CO_2 and 37 °C. Transfection reactions were prepared as follow: 3:2 ratio solution (3µg: 2µg) of pBKSII$^-$_LHA_mRuby_RHA and gRNA_Cas9_mCherry plasmids were added to 200 µL of CL medium + 200 µL of CL medium with 3 µL FuGene; 200 µL of CL medium with 2.5 µL of Cas9_GFP plasmid + 200 µL of CL medium with 1 µL FuGene (as a positive control); and 400 µL of CL medium with 1 µL FuGene (as a negative control).

After one day of transfection the whole medium was changed for CL medium and 48h after transfection, cells were suspended with accutase, washed in wash medium, resuspended in 2i/LIF medium with 0.05 U/mL Penicillin and 50 pg/mL Streptomycin (Pen/Strep, **Gibco**, #15070-063) and sorted at the Imperial College London MRC Flow Cytometry Facility using mCherry expression. Single cell sorting was performed into 96 well plates with 2i/LIF + Pen/Strep medium, pre-coated with Laminin. 72h after transfection, the medium was changed for fresh 2i/LIF + Pen/Strep medium. Sorted clones were following expanded in 2i/LIF + Pen/Strep medium.

2.5.4. Positive clones' validation

2.5.4.1. Western Blot: Obtained clones were grown during two days with 10 µM Nutlin (expecting to increase p21 expression), in 6-well plate (**Nunc FALCON**), coated with Gelatin, harvested with accutase and washed once in PBS. Additionally, a hTert-RPE1 cell line treated with 1µM Nutlin was used as a positive control. To obtain whole cell lysates, cells were treated with 1X Tris-Glycine SDS Buffer (**Novex**, #LC2676) + 5 mM DL-Dithiothreitol solution (Sigma, #43816) in water and incubated at 99 °C for 10 min. Samples were separated by **Novex™ WedgeWell™** 4-20% Tris-Glycine Gel (#XP04205BOX) on 1X Tris-Glycine SDS Running Buffer (**Novex**, #LC2675) and then transferred hydrophobic polyvinylidene fluoride membrane (**Millipore**, #IPFL00010). Membranes were blocked with 25g Skim milk (**VWR BDH Chemicals**, #84615.0500) in 1X tris-buffered saline (TBS) including 0.0025g/mL Glycerol Reagent Plus (**Sigma Aldrich**, #G7757), at RT for 1h and then incubated, overnight at 4 °C, with p21 (1 µg/mL, **BD Biosciences**, #556430) and vinculin antibodies. Next, membranes were washed three times in 1X TBS with 0.1 µL/mL Triton™ X-100 (**Sigma Aldrich**, #X100) (TBST), 10 min. each time, and incubated with Anti-mouse/rabbit IgG, HRP-linked secondary antibody (**Cell Signalling Technology**, #7076 / #7074), for 1h at RT. To observe the antibody binding Clarity Western ECL Substrate Kit (1 Luminol Substrate:1 Peroxide Solution ratio, **Bio-Rad**, #1705060) was used and blots were exposed to Amersham ImageQuant 800 Western Blot Imaging System.

2.5.4.2. PCR: To analyse the incorporation of mRuby DNA in the genomic DNA, pellet from all clones were obtained and DNA was extracted with Monarch Genomic DNA purification Kit (**BioLabs**, #T3010), following the manufacturer's instructions. PCR was performed in a 25 µL reaction containing ~50 µg genomic DNA, 0.5 U Phusion HF DNA polymerase (**BioLabs**, #M0530L), 0.5 µM each *Cdkn1a* primer (**Table 2.2**), 0.2 mM dNTPs, 1x Phusion HF Buffer (**BioLabs**, #B0518S). The cyclin protocol was performed as following, with step 2 repeated for 30 cycles:

98°C 30 sec

98°C 10 sec, 66°C 20 sec, 72°C 60 sec

72°C 5 min

4°C, Hold

Table 2.2. Details of primers used for PCR.

Gene	Orientation	Primer sequence 5'- 3'	Annealing temperature (°C)	Reference
***mRuby* overhanging *Cdkn1a* homologous arm**	Forward	TCTGCAAGAGAAAACCCGGAGGA GGAAACAGCCTGATCAAAGAAAA	55	-
	Reverse	GCGGGGCTGCCGTGGGCACTCTAC CCTCCGCCCAGGCCGG		
Cdkn1a	Forward	CCTATAACTAACTCTGGGCGTTGG	66	-
	Reverse	GGATGATATCAGTAGGACTGTTCC		
Inner mRuby	Forward	CGATTTCTTCAAGCAGAGC	65	-
	Reverse	GTTGCTGGGAAAATTCACG		

3. Results

Diapause is a natural process that pauses the pre-implantation blastocyst's development. In the blastocyst when diapause is induced *in vivo*, it has been reported that after five days all the blastocyst's cells have paused their cell cycle[36]. Regarding these cells' metabolism, this pause of the cell cycle is reported to be a quiescent state[69–71]. *In vitro*, when blastocysts are induced to diapause, it has been reported that the ICM cells arrest in a G0/G1-phase and it has been suggested that this is mediated by p21[36,72]. However, when diapause is induced in mESCs by mTOR or c-Myc inhibition, it is proposed that diapaused mESCs either have a slower proliferation rate (mTOR inhibition)[38] or that cells arrest in G0/G1-phase (c-Myc inhibition), the latter of which cannot be maintained for more than one day[37]. Therefore, the question whether diapause is a cell cycle arrest; and if it is like quiescence or more like another state of cell cycle arrest remains unclear. Here, I want to evaluate **what are the changes in the cell cycle when mESCs are induced to diapause**, and **how diapause compares to other states of cycle arrest**. In addition, p21 has been shown to mediate quiescence in other cell lines and mediate G0/G1-phase cells retainment in diapaused blastocysts. Thus, I also want to evaluate **if p21 plays a role on inducing mESCs into diapause**.

To manipulate the cell cycle in ESCs, I used a number of cell cycle inhibitors and compared their effects with previously published models of diapause, such as mTORi[38]. Palbociclib binds in the CDK4/6 kinases ATP binding pocket, and thus inhibits CycD-CDK4/6 complex activity[73]. This inactivation blocks Rb phosphorylation, preventing G1 to S-phase transition[50]. G1 arrest can also be caused by Nutlin which inhibits MDM2-p53 interaction, stabilizing p53 and leading to an increase of

p21 levels. Nutlin can also induce cell cycle arrest in G2-phase[51]. mESCs have high activity of CDK2 throughout the cell cycle[74] thus, I also will test a CDK1/2 inhibitor to evaluate mESCs' sensitivity to it.

3.1. mESCs are less sensitive to Palbociclib than somatic cells

Since mESCs have unique cell cycle regulation, they might respond differently to cell cycle inhibitors compared with somatic cells, in which these inhibitors have been previously characterised. Thus, I performed a dose curve response to Palbociclib treatment in mESCs. The response to treatments was evaluated by measuring the percentage of cells that were EdU (5-ethynyl-2'-deoxyuridine) stained. The EdU molecule is a nucleoside analogue of thymidine that can be incorporated during active DNA synthesis, when cells go through S-phase. Thus, mESCs were treated with the different concentrations of Palbociclib, pulsed with EdU for 20 minutes before fixing and staining for EdU to identify which cells were in S-phase during that time (**Fig. 3.1.A**).

Palbociclib was used in five different concentrations (**Fig. 3.1.B,** represented with different colours), in three independent experiments (represented in different colour's transparency) with three replicates each. The mean of the percentages of EdU positive cells, from each independent experiment were calculated (with n=3). The three means were plotted and a mean±SD graph from them was obtained by Prism Software (**Fig. 3.1.B**). In this assay untreated cells had an average between 60-70% of cells going through S-phase. When cells were treated with Palbociclib at 10 µM, the percentage of cells going through S-phase was reduced ~48% and 57% for 24h and 48h of treatment respectively, relatively to untreated cells. Moreover, this was confirmed on visual inspection of representative images from 10 µM Palbociclib treated cells, where I also observed a reduction of number of cells stained with EdU (**Fig.3.1.C**).

In addition, 2i/LIF + Palbociclib cultures, colonies are less round and flatter (i.e., more two dimensional (2D)) than untreated colonies (**Fig. 3.1.C)**. Since it is reported that 2i/LIF medium maintains mESCs in a stable naïve pluripotent state, it is not expected to observe differentiation in cells cultured with this medium. Thus, the colonies shape being modified from the mESCs characteristic three dimensional (3D) to 2D may suggest that this is predominantly a morphologic phenotype, although the mechanism of this morphological change is unclear. Along with this, in somatic cells treated with Palbociclib, a flattened cell shape is associated with senescence state[75]. However, in mESCs when in quiescence, colonies seem to remain in a dome-shape, similar to untreated cells[76]. However, I observed very few or no cell death and cells do not show a larger sized nucleus, which would be expected if cells were in a senescent state[77].

These results suggest that mESCs are less sensitive to Palbociclib than somatic cells, which usually completely arrest at around 0.5 µM Palbociclib[73]. mESCs lower sensitivity to Palbociclib may be due to CycD complexing with CDK2, since mESCs have high activity of CDK2 throughout the cell cycle[58,78]. Additionally, mESCs in Palbociclib treatment seem to show a new morphology that may characterize a distinctive quiescence state. 10 µM Palbociclib showed the most significant effect on cells proliferating, so was the selected concentration used for the following experiments.

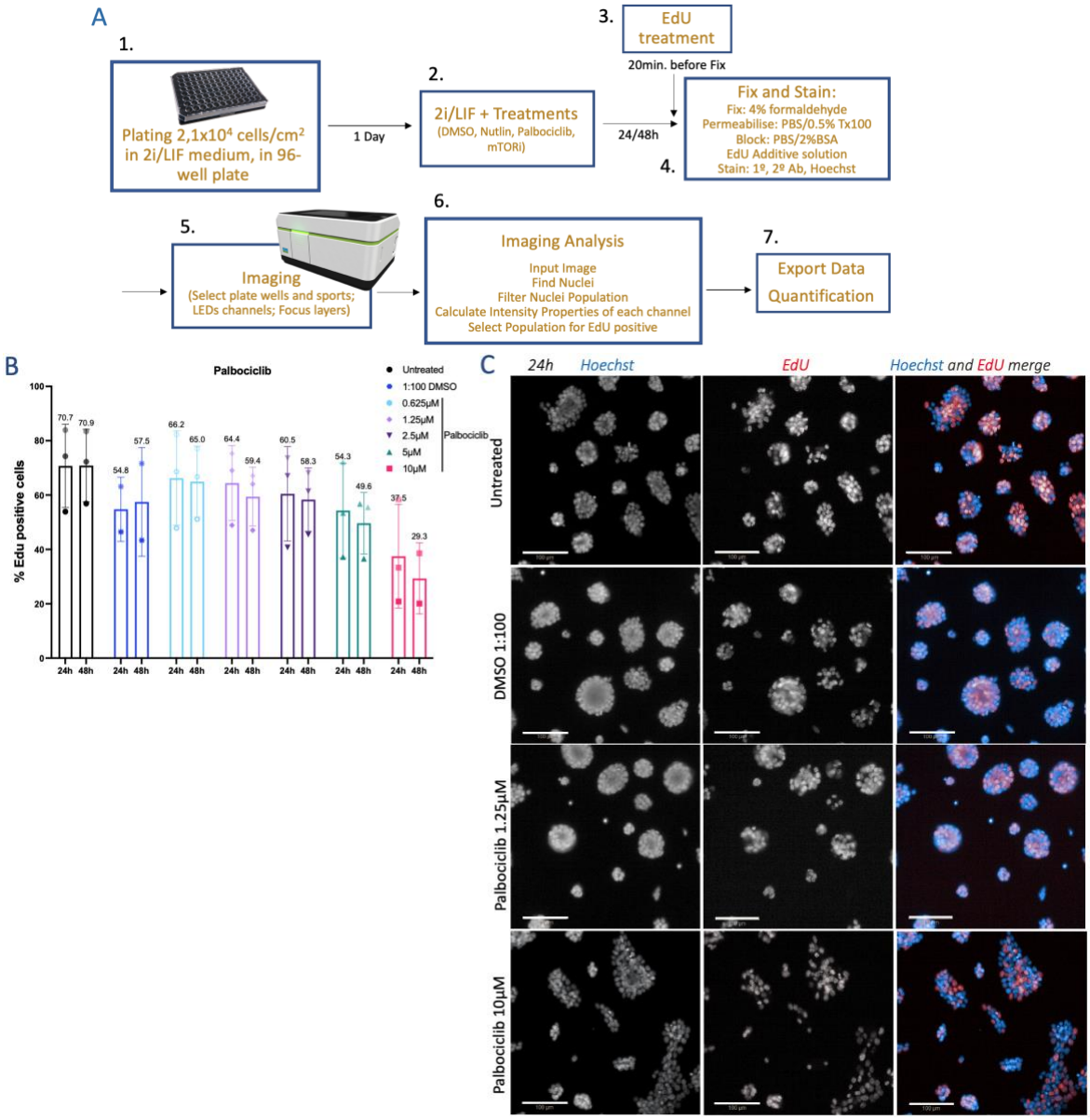

Figure 3-1. ***mESCs show sensitivity to Palbociclib treatment in high concentrations.*** *Cells were seeded and after 24h treated for untreated, DMSO and 0.625, 1.25, 2.5, 5 and 10 µM of Palbociclib conditions. After 24h/48h, EdU was pulsed for 20min. and cells were fixed, stained for Hoechst and EdU and imaged at 20x by Operetta microscope. Quantitative imaging analyses were performed in Harmony software, as in the workflow in* ***A****. Percentage of EdU positive cells were calculated directly by Harmony software with the number of EdU positive cells found in a well by this software and divided by the number of total nuclei found in the same well. Each concentration was tested in three independent experiments, with three replicates each; The mean of the percentage of EdU positive cells was calculated for each independent experiment.* ***B****- Plots with mean±SD from the calculated means of each experiment (n=3), per concentration of each time point; Concentrations are represented with different colours on the graph and each experiment is represented by different colour's transparency. Column bars represent the overall mean from the 3 experiments, on each concentration; Error bars represent SD;* ***C****- Images of E14 cells fixed and stained for Hoechst and EdU, in untreated, DMSO and 1.25 µM and 10 µM Palbociclib conditions. Scale bars are 100 µm.*

3.2. Paused and arrested mESCs present reduced colony growth, comparing with untreated cells

Colony forming assays were performed to evaluate the effect of cell cycle inhibitors on mESCs colony number per well and their growth. These observations might indicate if these inhibitors induce a cell cycle arrest or diapause-like state and if pluripotency is maintained. For this, colonies were stained

with alkaline phosphatase as a pluripotent cell marker[79], and after imaging with a zoom stereomicroscope (**Fig. 3.2.A**), the colonies were counted with the software Fiji.

Cultures treated with 0.2µM mTORi present reduced number of colonies comparing to DMSO treated ones, and also show a reduced colony size. In cultures treated with 10 µM Nutlin, similar results are observed. The mean number and size of colonies treated with Nutlin is significantly reduced, although less so than with mTORi treatment. By contrast, in Palbociclib-treated mESCs the number of colonies is similar to those treated with DMSO (**Fig.3.2.B**) but there is a significant reduction in colony size (although not as marked as in mTORi and Nutlin treated cultures) (**Fig.3.2.C**). When I visualized all wells, no alkaline phosphatase-negative colonies were found. Together these data show that mTORi and Nutlin inhibit cell growth while cells are maintained alive and pluripotent. Moreover, they show that Palbociclib has a less pronounced effect than Nutlin and mTORi in mESCs, and these cells continue growing although slower than 2i/LIF cultured cells. Together with the results above this suggests that although mESCs have lower sensitivity to Palbociclib than somatic cells, Palbociclib at 10 µM can affect mESCs proliferation rate. Perhaps, if higher doses would have been tested, Palbociclib would have had higher impact on mESCs growth like Nutlin and/or mTORi.

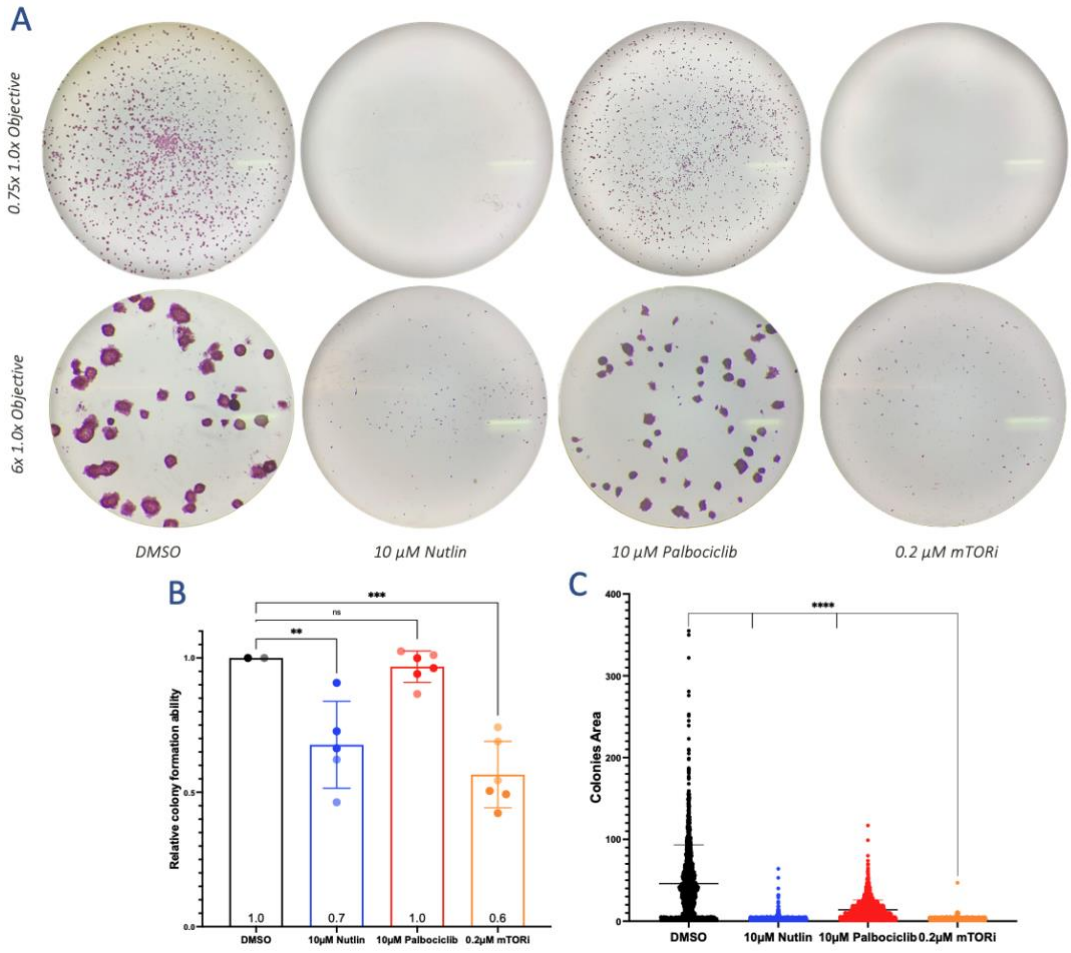

Figure 3-2 ***Representative images of colony formation assay.*** *Cells were seeded with 2 x 10^3 cells/well, in a 6-well plate, treated with DMSO, 10 µM Nutlin, 10 µM Palbociclib or 0.2 µM mTORi. After four days were fixed, stained for alkaline phosphatase and imaged with Leica stereomicroscope (**A**). Two independent experiments (different colour's transparency) each with two or three replicates were performed. The numbers and size of colonies were obtained with Fiji software. The mean number of colonies treated with DMSO were calculated per experiment and then normalized by its own value (for a relative value of one); The number of treated colonies, of each replicate, was normalized for the mean number of DMSO treated colonies of its experiment, to obtain its relative change value. Relative change values are represented in **B** in a mean±SD graph. Column bars represent the overall mean from the two experiments, on each condition; Error bars represent SD. In **C** is plotted area of colonies for the different conditions and its mean±SD. Statistical significance was obtained by*

*performing ordinary one-way ANOVA test. Asterisks indicate statistical significance compared to control (**p<0.01, ***p<0.001, ****p<0.0001), and **ns** meaning not significant.*

3.3. mESCs have a reduced fraction of cells in S-phase when treated with proliferation inhibitors

Following the previous results, I questioned whether the growth inhibition was due to slow proliferation rate or cell cycle arrest. To investigate this, I evaluated if the inhibitors were affecting the proliferation rate of mESCs by evaluating the proliferation fraction of mESCs treated with Nutlin, mTORi and Palbociclib for 24h and 48h. Untreated cells during 24h and 48h show a different percentage of cells going through S-phase, but not significantly. Cells that were treated with DMSO either for 24h or 48h show non-significant different means of EdU positive cells, comparing to their respective untreated condition. When treated with 10 µM Nutlin or 0.2 µM mTORi mESCs show a reduction in EdU positive cells of ~90% and ~80% for 24h and 48h respectively (**Fig. 3.3.A**). Whereas treatment with 10 µM Palbociclib decreased the percentage of cells in S-phase by ~ 60% and 50% at 24h and 48h respectively. When performing a visual inspection to compare with the automated analysis, I could confirm the quantitative results. Palbociclib, Nutlin and mTORi reduce the number of EdU positive cells (**Fig. 3.3.B**). This reduction is highest in mTORi, followed by Nutlin and lowest in Palbociclib treatment. This experiment suggests that with both Nutlin and mTORi, mESCs either have very low proliferation rate or they arrest in the cell cycle. The lower sensitivity of mESCs to Palbociclib treatment is also once again evident. Together with results shown for the capacity to form colonies, these results suggest that when treated with Palbociclib, either the whole population of mESCs grow slower or mESCs present a fraction of cells arresting in the cycle while a fraction of cells continue proliferation with a low rate.

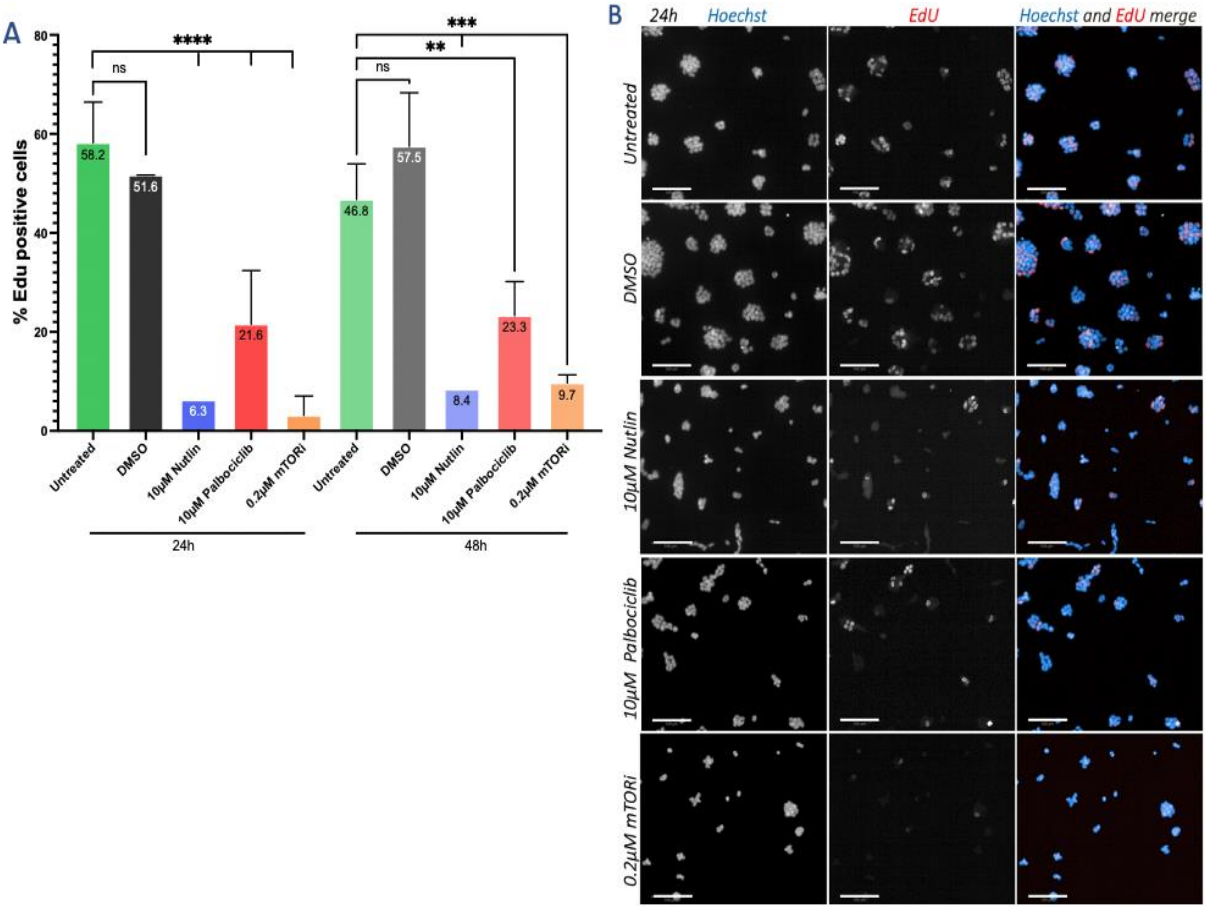

*Figure 3-3. **mESCs decrease S-phase-cells fraction when treated with proliferation inhibitors.** Cells were seeded and after 24h treated with respective condition. After 24h/48h, EdU was pulsed for 20min. and cells were fixed, stained for Hoechst and*

EdU and image at 20x by Operetta microscope. Imaging analyses were performed in Harmony software. Percentages of EdU positive cells were calculated directly by Harmony software with the number of EdU positive cells found in a well by this software and divided by the number of total nuclei found in the same well; ***A****- Plots with mean±SD from quantitative imaging data of EdU positive cells in % for untreated, DMSO, 10 µM Nutlin, 10 µM Palbociclib and 0.2 µM mTORi conditions, during 24h and 48h. Statistical significance was obtained by performing ordinary one-way ANOVA test. Asterisks indicate statistical significance compared to control (**p<0.01, ***p<0.001, ****p<0.0001), and ns meaning not significant.* ***B****- Images of E14 cells fixed and stained for Hoechst and EdU in untreated, DMSO, 10 µM Nutlin, 10 µM Palbociclib and 0.2 µM mTORi conditions. Scale bars are 100 µm.*

3.4. G0/G1-phase fraction cells increase with mTOR inhibition

After observing a decrease in EdU positive cells, I was wondering if cells were arresting in a specific cell cycle phase and if so, in which phase were they arresting. To analyse these questions and further confirm the previous results, I did a cell cycle profile analysis using Flow Cytometry. This assay is based on EdU (to stain cells going through S-phase) and Propidium Iodide (PI, that stains DNA content) staining of fixed cells (**Fig. 3.4.A**). Cells that are in G1-phase do not have EdU staining and have a low intensity of PI. When these cells enter early S-phase their DNA content is the same, and so is the PI intensity. However, in early S-phase cells start to incorporate EdU and so increase in its fluorescence. In late S-phase, cells have duplicated their DNA content and the PI intensity increases, presenting similar high intensity of EdU as early S-phase cells. After this, cells go into G2-phase, when their PI fluorescence level is doubled compared to G1-phase cells, and also cells in G2-phase do not incorporate EdU and so its fluorescence intensity is reduced comparing to S-phase cells.

Cells were cultured with untreated medium or with the different inhibitors for 24h and 48h, pulsed with EdU for 45 min., fixed and, after staining, analysed on a flow cytometer. After evaluation of intensities from the FACS analyser, the results were analysed by FlowJo software, the gates were created to define G0/G1- , S- or G2/M-phase cells (**Fig. 3.4.B**) and the percentage of cells in each phase, for each condition and for both 24h and 48h, were plotted (**Fig. 3.4.C**).

After 24h of treatment, ~30% untreated mESCs were in G1-phase, ~60% in S-phase and ~10% in G2-phase. When cells were cultured with inhibitors, I observed an increase of percentage of cells in G1-phase ~25% for mTORi and Palbociclib and ~50% for Nutlin treatments. S-phase cells fractions in this experiment decrease ~20% with mTORi and with Palbociclib and ~50% with Nutlin. While G2-phase % of cells are 1% and 3% reduced for Palbociclib and mTORi, respectively, Nutlin treated cells shown an increase of cells in G2-phase of ~5% (**Fig. 3.4.B and C**).

When cells were treated during 48h, the untreated condition shows ~53% of cells in G1-phase, ~40% in S-phase and ~5% in G2-phase. In the 2i/LIF + inhibitors cultures, I observed an increase of percentage of cells in G1-phase ~5, ~20, ~25% for Palbociclib, mTORi and Nutlin treatments, respectively. This increase is followed by a decrease in the % of S-phase cells, of ~7% with Palbociclib, ~15% with mTORi and ~25% with Nutlin. G2-phase % of cells, in this experiment, increase by 2% with Palbociclib and Nutlin and decrease 2% on mTORi treated cells, respectively (**Fig. S3.1 and Fig. 3.4.C**).

This experiment present similar results to those obtained by measuring the percentage of EdU positive cells with untreated and Nutlin treatment, for 24h, showing ~60% and ~10% of the cells were in S-phase, respectively. However, mTORi shows ~5% of EdU positive cells in the imaging experiment and ~40% of cells in S-phase with the FACS assay, meanwhile in Palbociclib treatment I observed ~25% of EdU positive cells and ~40% with the FACS assay. When analysing untreated and Nutlin results, they could suggest that EdU pulse and EdU positive cells calculation is a robust assay, however this assay has different results to those shown with the FACS assay for Palbociclib and mTORi, so I cannot conclude that the EdU pulse and EdU positive cells calculation assay is robust. For this

conclusion, would be important to perform more replicates of the FACS assay and evaluate if Palbociclib and mTORi show the same results as in here. In studies where serum+mTORi is used to induced diapause in mESCs, it is reported that mTORi does not alter the cell cycle distribution[38]. However, in my experiments both assays and timepoints show that mTORi treatment increase G0/G1-phase cells which oppose previous study's results. These differences may be explained due to different culture medium between my experiments (in 2i/LIF) and the reported study (in serum).

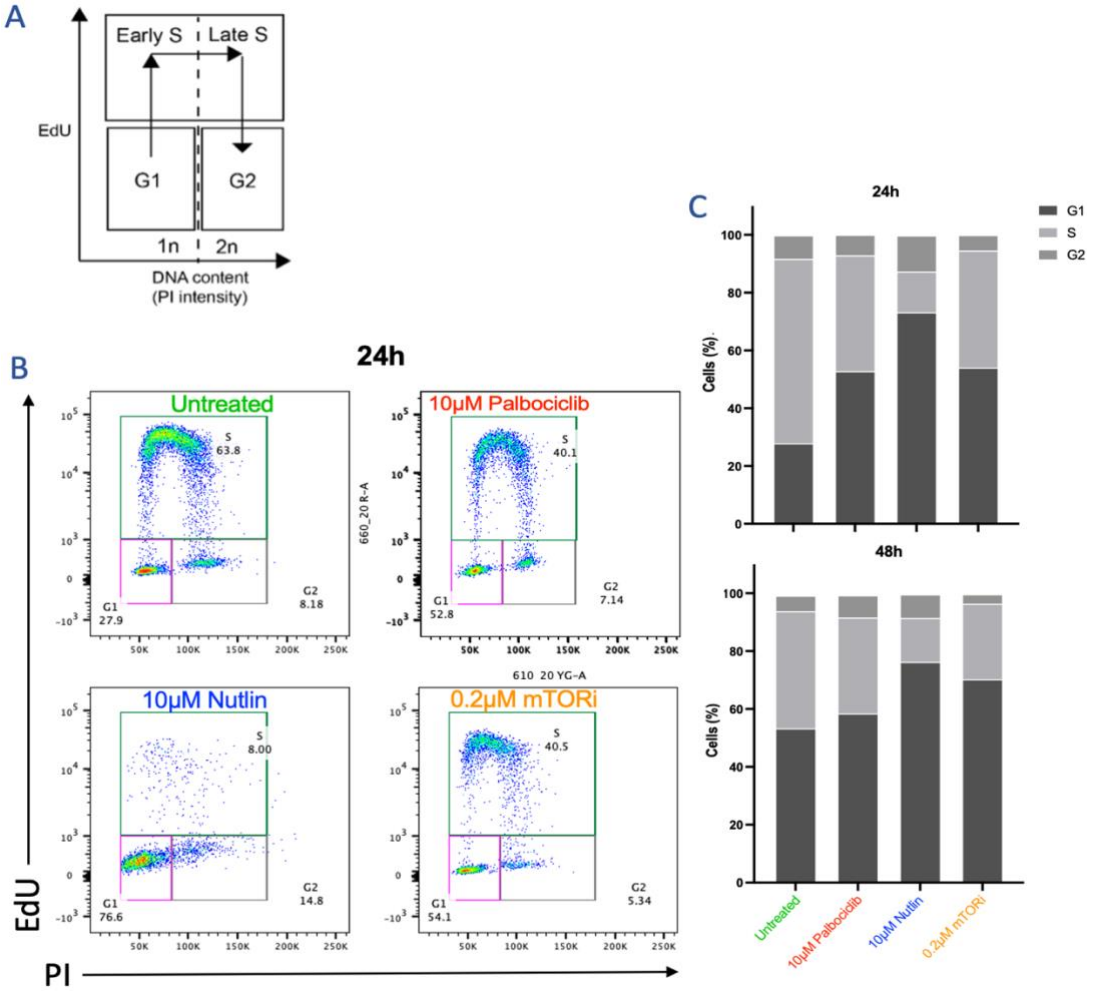

Figure 3-4. ***Proliferation inhibitors in mESCs increase G0/G1-phase fraction cells, as well as mTORi****. Cells were seeded and after 24h treated with respective condition. After 24h/48h, cells were pulsed for EdU, fixed, stained for EdU and PI and analysed by flow cytometry.* ***A****- Scheme explaining the correlation between the cell cycle progress and the intensities of both EdU and PI's (adapted from Malinowski, A., 2016* [80]*).* ***B****- Flow cytometry analysis of mESCs for 24h with all conditions.* ***C****- Histograms show proportions of mESCs are shown in one column bar per condition, for 24h (top graph) and 48h (bottom graph). Each column bar is formed with the percentage of cells in G1- (black), S- (light grey) and G2- (medium grey) phase of the cell cycle. The gates used to define cells at different cell-cycle stages are indicated in* ***B****.*

3.5. Nutlin and mTOR inhibitor decreased Cyclin D levels in mESCs

In mESCs when diapause is induced or other inhibitors are used, the studies only investigated if there are variations in the fraction of cells in the different cell cycle phases or whether the inhibitors induced differentiation. Thus, I was interested in evaluating differences in the levels of different cell cycle regulators when different cell cycle inhibitors or mTORi are used. Using quantitative immunocytochemistry imaging in treated and fixed cells, I evaluated CycD levels with and without

inhibitors. CycD is the first Cyclin that regulates the cell cycle and is described to be the only cyclin expressed with a peak of higher activity in G1-phase in mESCs[74].

CycD is downstream of mTOR and the point of regulation between growth signalling pathway and the cell cycle[81,82]. Therefore, I expected a decrease of CycD levels when mTOR is inhibited. Consistent with this, in my experiment, after 48h, images of stained anti-CycD antibody show lower levels of intensities in cells treated with 10 µM Nutlin and 0.2 µM mTORi (**Fig. 3.5.A**), compared with the controls. Regarding Nutlin treatment, it was reported that in a cancer cell line (MCF-7), the stabilization of p53 decreases CycD levels[83], it is theoretically possible a similar mechanism occurs here. By contrast, when 10 µM of Palbociclib was used to treat mESCs, CycD intensity values were similar to the values of untreated cells. When I plotted the obtained values of the CycD intensities distribution, I confirmed these results. CycD intensity levels decrease with Nutlin and mTORi treatments, while cells treated with Palbociclib have similar intensity values, compared with control conditions (**Fig. 3.5.B**).

Therefore, this experiment suggests, as expected, that CycD levels are downregulated when mESCs are induced to diapause and that a similar mechanism might be occuring between diapause and Nutlin-mediate arrest, since Nutlin decreases CycD levels and Palbociclib does not while both treatments cause mESCs arrest.

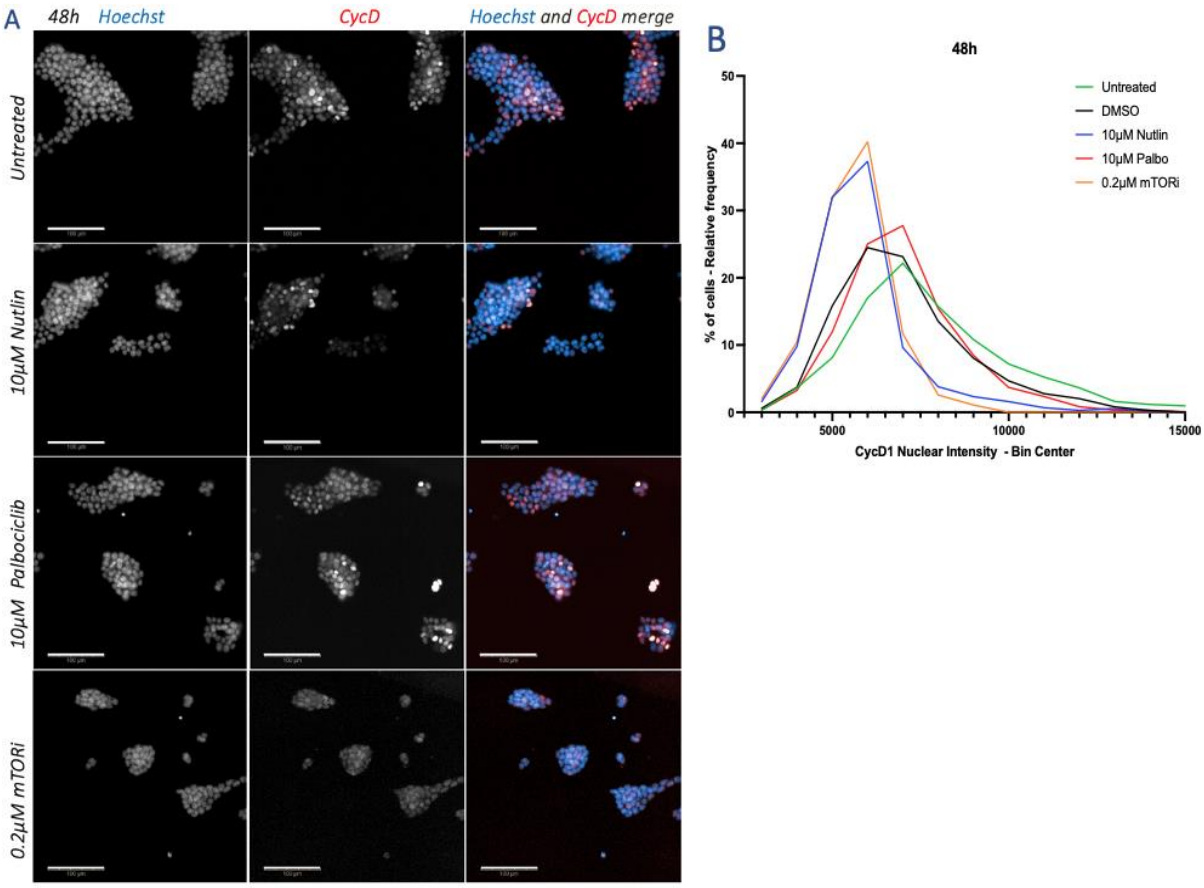

Figure 3-5. **Nutlin and mTOR inhibitor reduced number of nuclei and decreased Cyclin D levels in *mESCs***. *Cells were seeded and after 24h treated with respective inhibitors. After 48h, cells were fixed, stained for Hoechst and CycD and imaged at 20x by Operetta microscope.* **A**- *Images of E14 cells fixed and stained for Hoechst and CycD in untreated, 10 µM Nutlin, 10 µM Palbociclib and 0.2 µM mTORi conditions. Scale bars are 100 µm. Imaging analyses were performed in Harmony software. Intensity values of anti-CycD antibody were exported and analysed by Prism software. In* **B** *is represented the plot with relative frequency distribution of measured anti-cyclin D antibody intensities for each treatment - Untreated (green line) and DMSO (black line) as control conditions, Nutlin (blue line) and Palbociclib (red line) at 10 µM and mTORi (orange line) at 0.2 µM.*

3.6. Cell cycle inhibitors decrease phospho-RB levels in mESCs

In many cell cycle studies the level of Rb phosphorylation is used to evaluate if cells are arrested in G0-phase since in that stage Rb protein is hypophosphorylated[84–86]. Additionally, in mESCs it has been described that Rb is rapidly hyperphosphorylated permitting cells to cycle faster than somatic cells. Therefore, P-Rb levels could vary when diapause is induced and/or inhibitors of cell cycle are used and this might be informative as to the underlying molecular events.

For this, cells were cultured, treated with the different inhibitors for 48h, fixed and stained for phosphorylated Serine807/11-Rb (PS807/11-Rb) and phosphorylated Serine780-Rb (PS780-Rb). Although the time relation between these two phospho-sites is still not clear, it is suggested that phosphorylation of S780 occurs before phosphorylation of S807/811, since S780 phosphorylation has been proposed to be CycD-CDK4/6 complex specific whereas S807/811 phosphorylation is by both CDK4/6 and CDK2 complexes. I additionally stained cells for total Rb. Calculating a ratio of specific phospho-Rb per total Rb, potentially deletes any oscillation that the total Rb intensities might have. After staining, intensities from phospho-Rb/Rb ratio were plotted in a distribution graph.

After treating cells with mTORi, Nutlin and Palbociclib, for 48h, I observe a reduction of PS780-Rb protein levels in these three treatments, when compared to control conditions (**Fig. 3.6.A1**). Regarding PS807/11-Rb levels, mTORi decreases the intensities of this phosphorylation form in cells, compared with its levels in untreated cells. Although not as significant as mTORi, Palbociclib treated cells also show a reduction in phosphoS807/11-Rb levels. Whereas, when cells were treated with Nutlin, the distribution of PS807/11-Rb shows two peaks of intensities (**Fig. 3.6.A2**). Visual inspection of PS801/11-Rb's (here after mentioned as P-Rb) staining images confirms this finding (**Fig. 3.6.B**). Whereas a decrease of P-Rb intensities with Palbociclib treatment is observed, and a more marked decrease with mTORi; and for Nutlin treatment, cells with high intensity of P-Rb and other cells with low intensity are evident - in keeping with the distribution graphs.

During G1-phase, Rb protein is phosphorylated and later dephosphorylated during mitotic exit[87]. Thus, observing these two defined populations with different levels of P-Rb (i.e., two distinct peaks of intensity distribution shown) suggest that Nutlin arrests cells in distinct states in the cell cycle, perhaps early G1-phase and late G1- and/or G2-phase. This suggestion, coincide with previous results where S-phase fraction of cells decreases while the percentage of cells in G1- and G2-phase increase, with Nutlin treatment. Moreover, these results show that Rb is less phosphorylated when mESCs are treated with cycle inhibitors and with mTORi, and together with previous data, they suggest that mESCs may be arrested in G0/G1-phase when diapause is induced with mTORi. Also, since Nutlin and mTORi have similar percentage of cells in S-phase, decreased P-Rb levels (for cells in early G1-phase) and specially the common decreased of CycD, together these results may suggest similar mechanisms of regulation, between arrested (Nutlin treated) and diapaused (mTORi treated) cells.

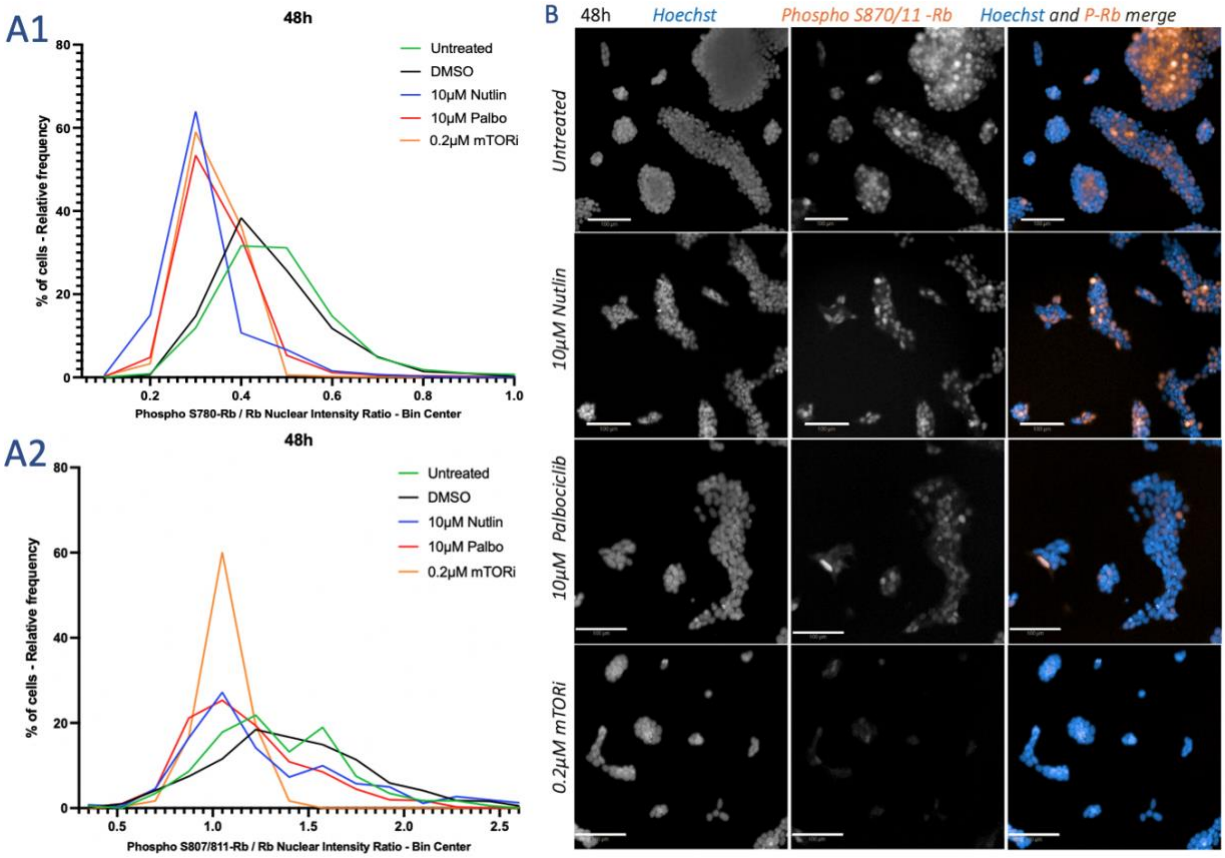

Figure 3-6. **Cell cycle inhibitors decrease phospho-RB levels in mESCs**. *Cells were seeded and after 24h treated with respective condition. After 48h, cells were fixed, stained for Hoechst, phosphoS807/11-Rb, of phosphoS780-Rb and total Rb and imaged at 20x by Operetta microscope. Imaging analyses were performed in Harmony software. Intensity values of anti-phosphoS780-Rb, anti- phosphoS807/11-Rb and anti-total Rb antibodies were exported and analysed by Prism software.* **A**- *Plots with quantitative imaging data from relative frequency distribution of anti- phosphoS780-Rb* ***(1)*** *and anti-phosphoS807/11-Rb* ***(2)*** *antibodies intensity, normalized by the intensity of total Rb, for each treatment - Untreated (green line) and DMSO (black line) as control conditions, Nutlin (blue line) and Palbociclib (red line) at 10 μM and mTORi (orange line) at 0.2 μM;* ***B***- *Images of E14 cells fixed and stained for Hoechst and phosphoS870/11-Rb in untreated, 10 μM Nutlin, 10 μM Palbociclib and 0.2 μM mTORi conditions. Scale bars are 100 μm.*

3.7. mESCs are sensitive to low concentrations of CDK1/2 inhibitor

In somatic cells, it has been suggested that one way cells may become less sensitive to Palbociclib is by complexing CycD with CDK2[88–90]. Increasing Palbociclib's concentration to 10 μM did impact mESCs proliferation. However since Palbociclib did not affect CycD levels, I was interested in testing mESCs sensitivity to a CDK2 inhibitor, especially since mESCs present high activity of CDK2 during the whole cell cycle[58,78]. Following this, I tested 7 different concentrations of CDK1/2 inhibitor III: 0.078, 0.156, 0.313, 0.625, 1.25, 2.5 and 5 μM, during 24h treatment. In this experiment, treated cells with CDK1/2i are flatter and have bigger nuclei (**Fig. 3.7.A**) which has been suggested to be a characteristic of arrested cells[75].

In addition, when CDK1/2i is used at 0.156 μM (**Fig. 3.7.B**), I observed an average of 6.5% ±3.0 of cells going through S-phase, suggesting that cells were almost completely arrested at 0.156 μM CDK1/2i. CDK1/2i at 0.312 μM also shows close to completely cell arrest (with 1.1% of cells in S-phase). However, at this concentration a high number of very small foci with high intensity of Hoechst (in blue), reminiscent of apoptotic bodies, are observed (**Fig. 3.7.A,** shown by arrow heads). Thus, 0.156 μM would be a good concentration to use in further experiments to induce cell cycle arrest in mESCs,

since it shows a low number of apoptotic bodies and very few cells in S-phase. Moreover, mESCs show 30% of cells proliferating with 0.078µM of CDK1/2i which represents 50% repression of the proliferation percentage from untreated cells (untreated cells show 60% of cells in S-phase). Since in somatic cells the IC_{50} for proliferation suppression is between 0.02 and 0.09 µM[91], this experiment suggests that mESCs do not have higher sensitivity to CDK1/2i than somatic cells.

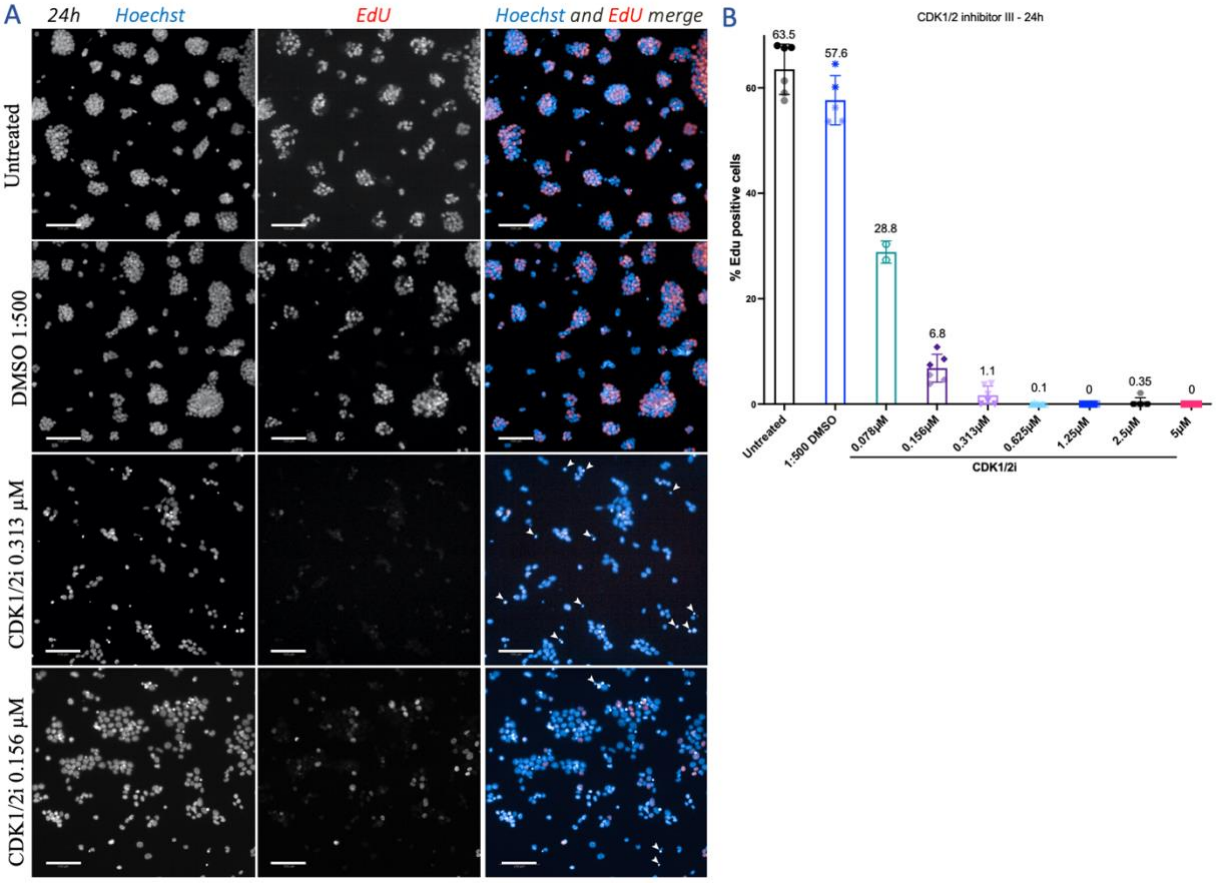

Figure 3-7. ***mESCs show sensitivity to CDK1/2 inhibitor even at lower than 1 µM.*** *Cells were seeded and after 24h treated with respective condition. After 24h, EdU was pulsed for 20min. and cells were fixed, stained for Hoechst and EdU and imaged at 20x by Operetta microscope. Imaging analyses were performed in Harmony software.* ***A****- Images of E14 cells fixed and stained for Hoechst and EdU, in untreated, DMSO and 0.313 µM and 0.156 µM CDK1/2i conditions. Arrow heads represent apoptotic bodies. Scale bars are 100 µm. Percentages of EdU positive cells were calculated directly by Harmony software with the number of EdU positive cells found in a well by this software and divided by the number of total nuclei found in the same well; Each concentration (represented with different colours) was tested in two independent experiments (represented with different colour's transparency), with three replicates each;* ***B****- Plots with mean±SD from quantitative imaging data of EdU positive cells in % for untreated and 0.078, 0.156, 0.313, 0.625, 1.25, 2.5 and 5 µM concentration of CDK1/2i, during 24h. Column bars represent the overall mean from the two experiments, on each concentration; Error bars represent SD;*

3.8. Generating a p21-mRuby mESC line

As mentioned previously, p21 is reported to be down regulated permitting mESCs rapid proliferation and in somatic cells it is one of the mediators of quiescence, downstream of replication stress. In blastocysts induced to diapause it has been suggested that p21 is upregulated and retains cells in G0/G1-phase. However, p21 function when mESCs enter and exit the induced diapause-like stage has not been studied. To help understand this regulation, it would be interesting to track p21 expression with a fluorescence tag, in real time when mESCs enter, remain in, and exit diapause. To do this, I aimed to use CRISPR/Cas9 engineering to incorporate an mRuby fluorophore into the C-terminal end of the gene encoding p21 (*Cdkn1a*) in mESCs. This incorporation results in the expression of p21 protein fused with a red fluorescent protein.

To perform this transfection, I constructed a plasmid with mRuby cDNA incorporated within homology regions to *Cdkn1a* C-terminal end. This plasmid was used together with a plasmid that had the CRISPR/Cas9 cassette and sgDNA needed for the desired incorporation. This second plasmid had also a mCherry cDNA, that encodes a red fluorescent protein. After two transfections with efficiency lower than 1%, positive single cells were sorted for red fluorescence. From sorting cells, I obtained and tested 70 single-cell clones.

To evaluate if the obtained clones had p21 tagged with mRuby, I visualized the clones under the Operetta microscope, in real time. Since p21 is expressed at a low level in mESCs and would be hard to detect, I analysed both untreated and Nutlin conditions, expecting to have an increase of p21 levels with Nutlin treatment (**Fig. 3.8.A**). When treated with Nutlin, non-transfected E14 cells, i.e., control without mRuby, had an increase of fluorescence. Although a background correction of the intensity was applied, this fluorescence may still represent elevated background. This made positive clones (i.e., clones that had mRuby's gene incorporated) difficult to identify when comparing to the control. Despite this, four clones had higher intensity of fluorescence, that appeared to be localised in the nucleus, being defined as potential positives.

Another way I used to evaluate if the clones were positive was by western blot and staining with anti-p21 antibody. As mentioned before, p21 is expressed at a low level in mESCs, and so I used untreated (**Fig. 3.8.B**, samples **(C)**) and treated with Nutlin (**Fig. 3.8.B,** samples **(N)**) cells from the clones to perform the western blot. Additionally, I used a hTert-RPE1 cell line treated with Nutlin, as a positive control for p21 labelling with the anti-p21 antibody (**Fig. 3.8.B**, sample **RPE1(N)**). p21 protein is reported to be ~20 kDa of weight, and when fused with mRuby is expected to increase its weight to ~46 kDa. When I imaged the western blot, I could not detect any promising band that would represent p21 neither in non-transfected E14 cells (**Fig, 3.8.B**, samples **Wt**) or on any clone samples (**Fig, 3.8.B**, samples **B6** and **H6**). However, both vinculin potential bands at ~124 kDa (positive control, to check if western blot was well performed) from all mESCs or p21 (~20 kDa) and vinculin (~124 kDa) from RPE1 control cells were observed in the western blot results.

To confirm whether I had successfully incorporated mRuby into the *Cdkn1a* gene, I performed a genomic DNA PCR, to amplify part of this gene together with mRuby (**Table 2.2** and **Fig. 3.8.C)**. p21 untagged amplified segment with these primers would have ~560 bp while p21-mRuby DNA would present ~1250 bp. From this method, I did not observe any bands in the PCR result from the negative control (H_2O). At the same time, I observed a PCR product ~1200-1500 bp and ~500-600 bp from the positive controls' samples (plasmid DNA - plasmid used to transfect, with p21 homologous regions and mRuby DNA -, and genomic DNA from untransfected E14 cells, respectively). Overall, one clone (**Fig. 3.8.D**, sample H6) shows 3 interesting PCR products (bands 1,2 and 3), with ~500-600 bp, ~600-700 bp and ~1200-1500 bp of size. Additionally, I redid a second PCR for H6 sample, where these results were confirmed (**Fig. S3.2**, sample H6). Therefore, H6 clone remains a potential heterozygous positive clone, and to confirm this would be interesting to sequence its three interesting PCR products, and analyse their sequence against the LHA-mRuby-RHA plasmid, used for mRuby incorporation during the transfection, and the whole mouse genome, to identify if H6 clone has mRuby incorporated in the *Cdkn1a* gene.

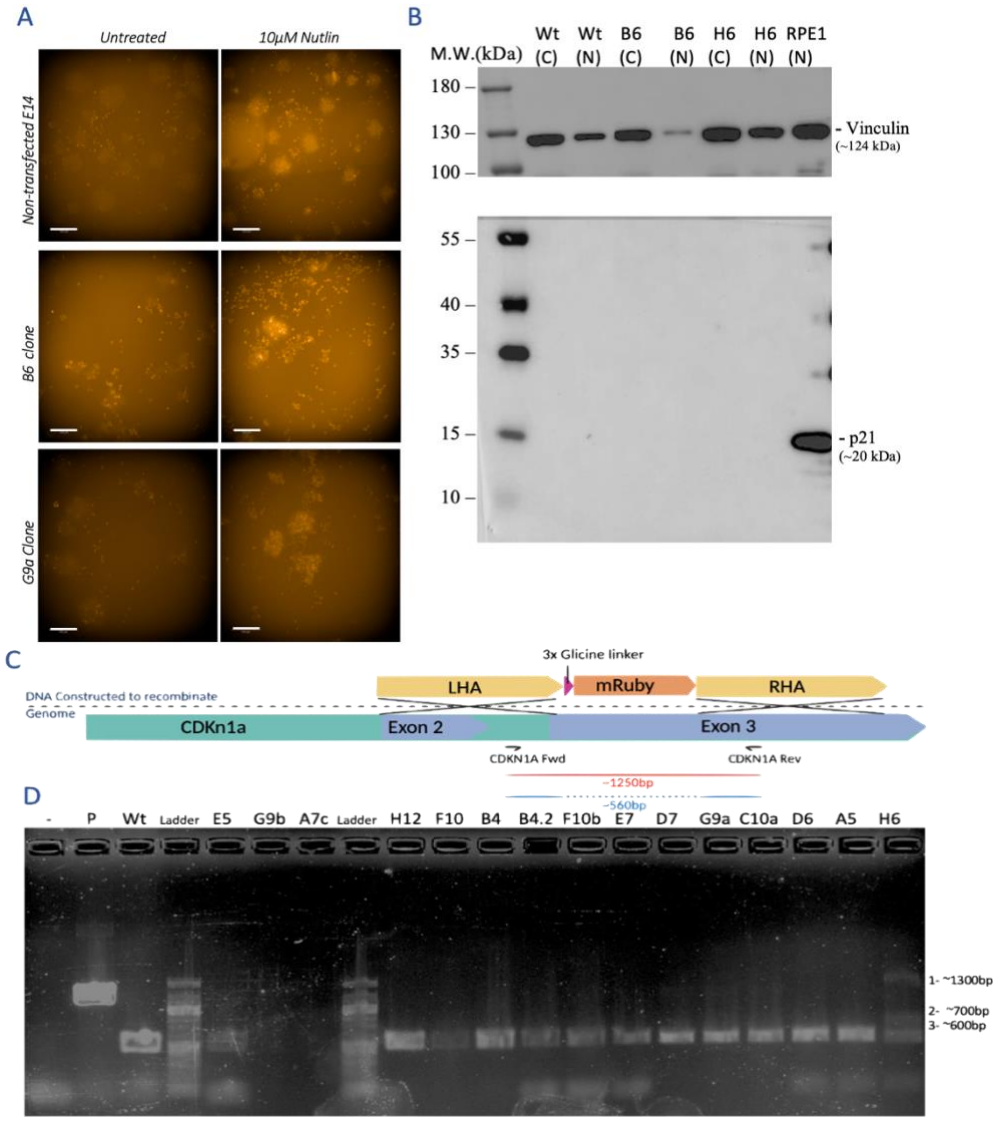

Figure 3-8. ***Transfected mESCs evaluation results show a potential heterozygous. A-*** *Untransfected and clones' cells were seeded and after 24h treated with or without Nutlin medium. After 24h, cells were imaged for 647nm fluorescence by operetta microscope. Scale bars are 100 µm.* ***B-*** *Lysates from untransfected cells (Wt) and clones (B6 and H6) treated for 24h with (N) and without (C) 10µM Nutlin and from RPE1 cells treated with Nutlin were obtained. These samples were submitted to western blot assay and the blot was incubated against anti-p21 and anti-vinculin antibodies. After staining, membranes were imaged by Amersham ImageQuant 800 Western Blot imaging system. p21and vinculin proteins were detected as a band with ~20 kDa and ~124 kDa, respectively. Bands with M.W. of ~80-90 kDa is a possible unspecific target form vinculin antibody. A molecular weight (M.W. in kDa unit) standard is presented on the side of the blot.* ***C-*** *Scheme of the insertion of left homology arm-3xGlicine-mRuby-right homology arm into Cdkn1a gene; CDK1NA forward and reverse (Table 2.2) were used to perform the PCR and genotype the clones.* ***D-*** *1% of agarose gel electrophoresis of PCR products for Cdkn1a primers. (-) lane refers to the negative control performed with H_2O; P is PCR product against plasmid DNA (plasmid with p21 homologous regions and mRuby DNA); Wt refers to genomic DNA from untransfected E14 cells resultant from the PCR. A 100 bp ladder was loaded in both lanes called "ladder". Other lanes are the PCR product from the PCR against the Clones genomic DNA.*

4. Discussion

In this project, I investigated regulation of the cell cycle in mouse embryonic stem cells (mESCs) and how the cell cycle changes when these cells enter a diapause state, *in vitro*. In cultures where diapause is induced, mESCs growth is suppressed. Growth arrest is accompanied by an increase in cells in the G0/G1-phase and a decrease in phosphorylated Rb and Cyclin D, G1-phase progression regulators. I used the cell cycle inhibitors Nutlin and Palbociclib to compare results between cell cycle arrested

mESCs and diapaused mESCs. Here, I suggest that mTORi treatment promote G1-phase arrest in mESCs. Additionally, I produced a cell line of mESCs that is potentially heterozygous for a p21-mRuby fusion protein.

4.1. CycD-CDK2 complex may mediate mESCs resistance to Palbociclib

Mouse ES cells exhibit the morphology, molecular homogeneity and transcriptome of naïve pluripotency, *in vitro,* in 2i/LIF medium[26,27]. Naive pluripotent stem cells have a faster cell cycle, which permits rapid self-renewal. The cell cycle regulation of these naïve pluripotent cells is poorly understood, as is the response to cell cycle inhibitors. Palbociclib is a CDK4/6 inhibitor which inhibits CycD-CDK4/6 complex activity and is usually used at 0.5 µM to completely arrest somatic cells[73]. Here, I demonstrated that mESCs are less sensitive of Palbociclib than somatic cells, and present a reduction of ~50% of the cells cycling with 10 µM of Palbociclib, relative to the control cells. In humans, it has been reported that CycD can complex with CDK2[88] and demonstrated that, in cancer cells *in vitro* resistance to CDK4/6 inhibitor is associated with increase of CDK2 activity[89,90]. These findings together with my results, and the high levels of CDK2 activity throughout the cell cycle already reported in mESCs, may suggest that mESCs are resistant to Palbociclib due to CycD-CDK2 complex permitting cell cycle progression. Moreover, I show that in mESCs CycD levels are maintained when Palbociclib treatment is used. This result is not surprising since Palbociclib binds to CDK4/6 kinases inhibiting their activity, and does not directly interact with CycD. Co-treatment of Palbociclib with inhibition of CycD-upstream-pathways, such as oestrogen[92] or mTOR[93] inhibition, has been suggested as one strategy to overcome this resistance.

Showing that mESCs are less sensitive to Palbociclib, reinforces the idea that mESCs have a unique cell cycle regulation, perhaps with mechanisms that reinforce cell division, such as the presence of alternative complexes (e.g., CycD-CDK2). This might indicate a common mechanism with some cancer cell lines. Additional experiments to assess if CycD-CDK2 is the alternative complex used by mESCs to resist Palbociclib would be interesting to test this hypothesis. For example, experiments that examine CycD-CDK2 affinity in these cells followed by evaluation of CycD-CDK4/6 and CycD-CDK2 complex levels in Palbociclib treated mESCs.

Additionally, after observing mESCs resistance to Palbociclib, I investigated how these cells respond to CDK1/2 III inhibitor. Previous, I discussed that CDK2 may be the alternative pathway through which mESCs are resistant to Palbociclib treatment. Also, it has been reported that CDK2 has high activity through the whole mESCs cycle[58,78] so, it is expected that these cells are similarly or more sensitive than somatic cells to CDK1/2i. In somatic cells, CDK1/2i has an IC_{50} of growth inhibition between 0.02 µM – 0.09 µM[91]. In my experiments, I show that CDK1/2i reduces ~50% of proliferation at 0.078 µM, compared to the control. Thus, mESCs show a similar sensitivity to this inhibitor as somatic cells. Although this experiment does not test if CDK2 is the alternative pathway for Palbociclib resistance, it informs us how sensitive mESCs are to CDK1/2 inhibitor. In future experiments would be interesting to test the use of a low dose of Palbociclib with a low dose of CDK1/2 inhibitor to see if that induces cell cycle arrest more than the CDK1/2 inhibitor alone. This would suggest that Palbociclib resistance is potentially mediated by CycD-CDK2 complexes.

4.2. Naïve mESCs do not differentiate up to four days of Nutlin treatment

Further analysing the cell cycle inhibitors' effects on mESCs cultures I performed a colony formation assay and stained the colonies for alkaline phosphatase. Alkaline phosphatase is used as a

pluripotent cells marker[79] in this assay. Although mESCs are less sensitive to Palbociclib, here I show that their growth is significantly reduced while their pluripotency is maintained. These results confirm that not all cells arrest in the cell cycle with Palbociclib treatment. Additionally, it would be interesting to test higher doses and/or daily addition of Palbociclib to evaluate further sensitivity. On the other hand, my experiment shows that with either mTORi or Nutlin, a large reduction of the colonies' growth occurs, while maintaining their pluripotency. mTORi is used here as a model of induced diapause, as already reported[38]. Thus, my results are consistent with this study, suggesting that mTORi does not perturb pluripotency while inducing diapause in mESCs, and that diapause can be elongated for days, specifically in my experiment up to four days. However, it has been demonstrated that p53 is a negative upstream factor of Nanog (an important pluripotency gene)[94], and also that mESCs express higher basal levels of p53 than somatic cells[95]. The higher levels of p53 in mESCs might be expected to lead to Nanog downregulation, destabilizing pluripotency. However, this apparent contradiction has been explained by the report of p53 localization in the cytoplasm and its reduced ability to translocate to the nucleus in mESCs[63,64]. Nutlin is used as a p53 activator to study cell cycle and in particularly to increase p21, to study the G1 checkpoint and cell cycle arrest. In mESCs, when Nutlin was used at 10 μM for three days, it was reported that these cells undergo a differentiation process[65]. In my experiment, Nutlin was supplemented to 2i/LIF medium at 10μM for four days and I show that mESCs maintain their pluripotency, which oppose the previous findings. However, Suvorova, and colleagues report that mESCs differentiate when Nutlin is supplemented in serum+LIF, whereas 2i/LIF medium stabilizes mESCs in the naïve pluripotency state, blocking differentiation[96,97].

Therefore, together these findings suggest that the medium in which mESCs are cultured plays an important role when studying the cell cycle regulation in these cells. Since different culture mediums maintain mPSCs in a different pluripotent state, parallel experiments with these different mediums are required to study each state and to compare them. Although, I demonstrated here that naïve pluripotent mESCs cultured in 2i/LIF do not differentiate with Nutlin up to four days, the mechanism by which the growth in these cells is reduced is still unclear and merits further investigation.

4.3. mTOR inhibition increase G0/G1-phase fraction cells in naïve mESCs

The growth reduction observed in my experiments when cells are treated with inhibitors, can be due two reasons 1) mESCs proliferation rate is reduced; or 2) inhibitors induce an arrest of the cell cycle in mESCs. To answer this question, I analysed the percentage of cells going through S-phase and the cell cycle of treated mESCs. Based on my findings I conclude that Palbociclib is retaining majority of the cells in G0/G1 phase and Nutlin is arresting mESCs in G0/G1- and G2-phase. Although these treatments have not previously been used in naïve mESCs culture (i.e., in 2i/LIF medium), they are usually used in somatic cell lines culture to study their cell cycle. Palbociclib is strongly related to retaining cells in G1-phase[98] and Nutlin usually blocks cell cycle progression in G1- and in G2-phase[99,100]. As mentioned above, Palbociclib inhibits CDK4/6 activity which is a G1-phase regulator and so, cells are inhibited to progress in G1-phase. However, Nutlin is a p53 activator that consequently increases p21 expression. In its turn, p21, is a cell cycle progression inhibitor, since it inhibits CDK4/6 and CDK2 activity which are G1- and G2-phase regulators, respectively[52]. Therefore, Nutlin can inhibit cells to transit from G1-phase and from G2-phase.

On the other hand, the inhibition of mTOR supplemented to 2i/LIF medium is reported to induce a diapause-like state[38]. However, diapause induced stage in mESCs is poorly understood, especially its cell cycle regulation. In independent studies, the cell cycle has been reported to either slow or pause completely. In my experiments with 2i/LIF+mTORi medium, I reproduced the mESCs'

reduction of growth rate, as in the previous study[38], while maintaining their survival and pluripotency. I also suggest that mESCs colonies' growth progressively reduces over time and is due to arrest of cells in G1-phase. These results contrast with the previous study where it is described that mTORi only affects mESCs' proliferation rate, without arresting in any cell cycle phase[38]. However, Bulut-Karsliogluand colleagues use serum + mTORi medium to evaluate diapaused-mESCs' cell cycle. Thus, this disagreement may be due to differences in medium. Moreover, serum mESCs likely represent a later stage of development, closer to implantation. Regarding this, if diapause induction at early stages of development leads to cell cycle arrest and at later stages only slows proliferation rate, this may suggest that an unknown mechanism is activated during this time that does not allow cell cycle arrest. Perhaps, a mechanism related to the more marked lack of the restriction-point in primed pluripotent cells[74]. Therefore, this may suggest that diapause gets more difficult to induce as the embryo reaches the implantation process and becomes impossible post implantation. It has been described that primed human ESCs (hESCs) are similar to mouse post-implantation epiblast-derived stem cells (mEpiSCs)[101,] whereas the more recently described naïve hESCs reassemble ICM's cells from the human blastocyst at day 6-7's[102,103], which are similar to naïve mESCs[104]. Therefore, studying naïve mESCs' cell cycle regulatory pathways and either compare them to mEpiSCs or directly to naïve hESCs may further inform our knowledge in hESCs, at both cell cycle and diapause levels, and allow future studies into whether diapause might be possible in humans.

Together with these findings, my results suggest that Palbociclib and Nutlin arrest the mESCs cell cycle in the same phases as in somatic cells. Also, I demonstrate that 2i/LIF+mTORi arrest the mESCs in G1-phase, in contrast to previous studies which demonstrate that serum+mTORi only reduces mESCs proliferation rate. This reinforces the idea that it is important to consider both the appropriate medium and the particular stage of pluripotency, when studying mPSCs.

4.4. Diapaused mESCs present low levels of CycD and phosphorylated Rb

Due to the lack of knowledge about regulators of the cell cycle in mESCs, I proceeded to analyse the levels of some key cell cycle regulators. The early stages of the cell cycle are regulated mainly by the CycD-CDK4/6 complex, which phosphorylates Rb protein permitting G1- to S-phase transition. Thus, analysing CycD and/or P-Rb is of interest to investigate how cells regulate their cycle while arresting.

As I discussed previously, Palbociclib does not interact directly with CycD and so in mESCs the levels of CycD are maintained compared with the control. In agreement with this, reported studies with human cancer cell lines, such as MCF-7 (a human cancer cell line), CycD levels are also not affected when Palbociclib is in culture[105]. Moreover, CycD has previously been described to have higher expression in cancer lines, such as MESO[106] and HCT116[107], when treated with Nutlin. This is mainly associated with CycD forming a complex with MDM2, while complex formation with p53 is inhibited by Nutlin. However, in MCF-7 treated with Nutlin it is shown that CycD levels decrease[83]. Consistent with this, my experiments show that CycD expression is reduced when mESCs are treated with Nutlin. In addition, with mTORi treatment mESCs show reduction of CycD levels while arresting in the cell cycle. This may not be surprising as mTOR is proposed as an upstream positive regulator of CycD[81]. However, this may suggest that downregulation of CycD is necessary for mESCs arrest, during diapause although it does not demonstrate if it is sufficient. This also may suggest that co-treatment of Palbociclib and mTORi might overcome the issue of tumour resistance to CDK4/6 inhibitors, as discussed previously. In addition, it was reported that overexpression of microRNA let-7 induces diapause in mESCs[39], also downregulates CycD in the MCF-7 cell line[83]. Together these results show an association

between decreased CycD levels and the induction of arrest and diapause in mESCs. They also suggest that mESCs and MCF-7, share similar pathways in response to cell cycle inhibitors. This may be important for further studies, to compare mESCs' diapause with cancer dormancy.

My experiments show that the levels of phosphorylated Rb is reduced when mESCs are arrested in G1-phase (with Palbociclib) and diapaused with mTORi. Since Rb protein, in somatic cells, is dephosphorylated during mitosis and phosphorylated throughout G1-phase, this is an important mechanism (resultant from CycD-CDK4/6 activity) for G1 progression and S-phase entrance[46]. Therefore, the level of the phosphorylated form of the Rb protein is also an indicator that cells are arresting in G1 phase. I also found two subpopulations of Rb, hypophosphorylated and hyperphosphorylated populations, with Nutlin treatment which is consistent with arrest in early G1-phase and in latter G1- and/or G2- phases, respectively. Although it is expected that early G1-phase population have low levels of P-Rb, and late G1- and G2-phase population have higher phosphorylation of Rb[84–86] it is interesting to observe possible co-existence of these two populations in mESCs . In future studies, it would be interesting to do a FACS experiment to sort G1- and G2- phases after Nutlin treatment and perform a western blot with an anti- P-Rb antibody.

Together these results indicate that mESCs arrested in G1-phase and diapaused mESCs decrease CycD levels, except when Palbociclib is used, since it does not interact directly with CycD. In addition to the downstream regulation of CycD activity, but not surprisingly, P-Rb levels also decrease in G1-phase arrested and diapaused mESCs.

4.5. E14.p21-mRuby cell line was obtained to track p21's activity in real time

p21 has been suggested to be a mediator for cells retainment in G0/G1-phase, when diapause is induced in blastocysts[36,72]. However, p21's role in diapause mESCs has not been reported. Therefore, to bypass this lack in our knowledge, I transfected mESCs with CRISPR/Cas9, to incorporate mRuby (fluorescence protein) coding gene into *Cdkn1a* (p21's gene). From this assay, I hoped to obtain an mESCs cell line that reports p21 activity by its fusion with mRuby. I could not proceed to validation of this cell line and its application to evaluate p21 activity and role in mESCs cell cycle as they enter diapause, due to my thesis deadline approach. However, if successfully targeting is confirmed these cells will be important for future experiments to test the hypotheses if p21 plays a role in regulating the mESCs cell cycle while diapause is inducted. In addition, it is known that ESCs can be differentiated into other pluripotent stages and also into PGCLCs (primordial germ cell-like cells). Therefore, this p21 reporter cell line may also be important to understand and compare p21's activity between pluripotent states and also in PGCLCs. In addition, mESCs can be injected into blastocyst and contribute to chimeras[19–21], which might allow generation of a reporter mouse for *in vivo* studies.

5. Conclusions

Additional studies are necessary to understand how the mESC cell cycle is regulated. The role of p21 in the mESC cell cycle and in mouse diapause remains to be tested, as I was unable to analyse the p21 reporter cell line, while inducing diapause.

mESCs cell cycle is still poorly understood as well as the regulation of diapause, at the cell cycle levels, in these cells so, additional studies are necessary. However, here I have shown that mESCs are less sensitive to CDK4/6 inhibitors, possibly due to CDK2 high activity, and that this may be bypassed by arresting the cells with inhibition of CycD. And I also show that naïve mESCs can arrest

without differentiating with Nutlin treatment and arrest in G0/G1 when induced to diapause with mTORi.

In addition, my results suggest that CycD and P-Rb levels decrease in arrested and diapaused cells. In this regard, mESCs have similar response to inhibitors as the cancer cell line MCF-7. Further experiments would be important to understand if these similarities are significant and if they point towards shared mechanisms between these cell types that permit a diapause-like dormancy stage in cancer cells, as has been suggested previously[108].

Further experiments are required to evaluate if other Cyclins (as CycE and CycA) in the cell cycle are affected when mESCs are arrested or diapaused. Additionally, future studies could compare cell cycle regulation between different stages of pluripotency. This may inform if or how diapause occurs in humans, as mEpiSC are reported to be similar to hESCs[101] and naïve mESCs to naïve hESCs[104].

6. References

1. DeSesso, J. M. Embryotoxicity: Anatomical, Physiological, and Functional. in *Comprehensive Toxicology* 11–25 (Elsevier, 2010). doi:10.1016/B978-0-08-046884-6.01504-9.
2. Chambers, I. & Smith, A. Self-renewal of teratocarcinoma and embryonic stem cells. *Oncogene* **23**, 7150–60 (2004).
3. Niwa, H. How is pluripotency determined and maintained? *Development* **134**, 635–46 (2007).
4. Silva, J. & Smith, A. Capturing pluripotency. *Cell* **132**, 532–6 (2008).
5. Lepire, M. L. & Ziomek, C. A. Preimplantation Mouse Embryos Express a Heat-Stable Alkaline Phosphatase1. *Biol. Reprod.* **41**, 464–473 (1989).
6. Osorno, R. *et al.* The developmental dismantling of pluripotency is reversed by ectopic Oct4 expression. *Development* **139**, 2288–98 (2012).
7. Nichols, J. & Smith, A. Naive and Primed Pluripotent States. *Cell Stem Cell* **4**, 487–492 (2009).
8. Loh, K. M., Lim, B. & Ang, L. T. Ex Uno Plures: Molecular Designs for Embryonic Pluripotency. *Physiol. Rev.* **95**, 245–295 (2015).
9. Orkin, S. H. & Hochedlinger, K. Chromatin connections to pluripotency and cellular reprogramming. *Cell* **145**, 835–50 (2011).
10. Kinoshita, M. *et al.* Capture of Mouse and Human Stem Cells with Features of Formative Pluripotency. *Cell Stem Cell* **28**, 453-471.e8 (2021).
11. Hayashi, K., Ohta, H., Kurimoto, K., Aramaki, S. & Saitou, M. Reconstitution of the Mouse Germ Cell Specification Pathway in Culture by Pluripotent Stem Cells. *Cell* **146**, 519–532 (2011).
12. Kojima, Y. *et al.* The Transcriptional and Functional Properties of Mouse Epiblast Stem Cells Resemble the Anterior Primitive Streak. *Cell Stem Cell* **14**, 107–120 (2014).
13. Ohinata, Y. *et al.* A Signaling Principle for the Specification of the Germ Cell Lineage in Mice. *Cell* **137**, 571–584 (2009).
14. Tesar, P. J. *et al.* New cell lines from mouse epiblast share defining features with human embryonic stem cells. *Nature* **448**, 196–199 (2007).
15. Huang, Y., Osorno, R., Tsakiridis, A. & Wilson, V. In Vivo Differentiation Potential of Epiblast Stem Cells Revealed by Chimeric Embryo Formation. *Cell Rep.* **2**, 1571–1578 (2012).
16. Takahashi, K. & Yamanaka, S. Induction of Pluripotent Stem Cells from Mouse Embryonic and Adult Fibroblast Cultures by Defined Factors. *Cell* **126**, 663–676 (2006).
17. STEVENS, L. C. Embryology of testicular teratomas in strain 129 mice. *J. Natl. Cancer Inst.* **23**, 1249–95 (1959).
18. Stevens, L. C. The development of transplantable teratocarcinomas from intratesticular grafts of pre- and postimplantation mouse embryos. *Dev. Biol.* **21**, 364–82 (1970).
19. Mintz, B. & Illmensee, K. Normal genetically mosaic mice produced from malignant

teratocarcinoma cells. *Proc. Natl. Acad. Sci. U. S. A.* **72**, 3585–9 (1975).
20. Kaufman, M. H. & Evans, M. J. Establishment in culture of pluripotential cells from mouse embryos. *Nature* **292**, 154–156 (1981).
21. Martin, G. R. Isolation of a pluripotent cell line from early mouse embryos cultured in medium conditioned by teratocarcinoma stem cells. *Proc. Natl. Acad. Sci.* **78**, 7634–7638 (1981).
22. Brook, F. A. & Gardner, R. L. The origin and efficient derivation of embryonic stem cells in the mouse. *Proc. Natl. Acad. Sci.* **94**, 5709–5712 (1997).
23. Suda, Y., Suzuki, M., Ikawa, Y. & Aizawa, S. Mouse embryonic stem cells exhibit indefinite proliferative potential. *J. Cell. Physiol.* **133**, 197–201 (1987).
24. Hayashi, K., Lopes, S. M. C. de S., Tang, F. & Surani, M. A. Dynamic Equilibrium and Heterogeneity of Mouse Pluripotent Stem Cells with Distinct Functional and Epigenetic States. *Cell Stem Cell* **3**, 391–401 (2008).
25. Smith, A. Formative pluripotency: the executive phase in a developmental continuum. *Development* **144**, 365–373 (2017).
26. Wray, J., Kalkan, T. & Smith, A. G. The ground state of pluripotency. *Biochem. Soc. Trans.* **38**, 1027–1032 (2010).
27. Boroviak, T., Loos, R., Bertone, P., Smith, A. & Nichols, J. The ability of inner-cell-mass cells to self-renew as embryonic stem cells is acquired following epiblast specification. *Nat. Cell Biol.* **16**, 513–525 (2014).
28. Fenelon, J. C., Banerjee, A. & Murphy, B. D. Embryonic diapause: development on hold. *Int. J. Dev. Biol.* **58**, 163–174 (2014).
29. Renfree, M. B. & Fenelon, J. C. The enigma of embryonic diapause. *Development* **144**, 3199–3210 (2017).
30. RENFREE, M. B. Initiation of development of diapausing embryo by mammary denervation during lactation in a marsupial. *Nature* **278**, 549–551 (1979).
31. van der Weijden, V. A. & Ulbrich, S. E. Embryonic diapause in roe deer: A model to unravel embryo-maternal communication during pre-implantation development in wildlife and livestock species. *Theriogenology* **158**, 105–111 (2020).
32. WHITTEN, W. K. ENDOCRINE STUDIES ON DELAYED IMPLANTATION IN LACTATING MICE. *J. Endocrinol.* **13**, 1–6 (1955).
33. Ptak, G. E. *et al.* Embryonic Diapause Is Conserved across Mammals. *PLoS One* **7**, e33027 (2012).
34. YOSHINAGA, K. & ADAMS, C. E. DELAYED IMPLANTATION IN THE SPAYED, PROGESTERONE TREATED ADULT MOUSE. *Reproduction* **12**, 593–595 (1966).
35. Arena, R. *et al.* Lipid droplets in mammalian eggs are utilized during embryonic diapause. *Proc. Natl. Acad. Sci.* **118**, e2018362118 (2021).
36. Kamemizu, C. & Fujimori, T. Distinct dormancy progression depending on embryonic regions during mouse embryonic diapause†. *Biol. Reprod.* **100**, 1204–1214 (2019).
37. Scognamiglio, R. *et al.* Myc Depletion Induces a Pluripotent Dormant State Mimicking Diapause. *Cell* **164**, 668–680 (2016).
38. Bulut-Karslioglu, A. *et al.* Inhibition of mTOR induces a paused pluripotent state. *Nature* **540**, 119–123 (2016).
39. Liu, W. M. *et al.* Let-7 derived from endometrial extracellular vesicles is an important inducer of embryonic diapause in mice. *Sci. Adv.* **6**, (2020).
40. McLAREN, A. A STUDY OF BLASTOCYSTS DURING DELAY AND SUBSEQUENT IMPLANTATION IN LACTATING MICE. *J. Endocrinol.* **42**, 453–463 (1968).
41. Tarín, J. J. & Cano, A. Do human concepti have the potential to enter into diapause? *Hum. Reprod.* **14**, 2434–2436 (1999).
42. Wilde, M. H., Xie, S., Day, M. L. & Pope, W. F. Survival of small and large littermate blastocysts in swine after synchronous and asynchronous transfer procedures. *Theriogenology* **30**, 1069–1074 (1988).
43. ANNE McLAREN, D. M. Studies on the Transfer of Fertilized Mouse Eggs to Uterine Foster-Mothers. *J. Exp. Biol.* **33**, 394–416 (1956).
44. Joung, S. Y. *et al.* Effects of transferring in vitro -cultured rabbit embryos to recipient oviducts on mucin coat deposition, implantation and development. *Zygote* **12**, 215–219 (2004).

45. Nepomnaschy, P. A., Weinberg, C. R., Wilcox, A. J. & Baird, D. D. Urinary hCG patterns during the week following implantation. *Hum. Reprod.* **23**, 271–277 (2007).
46. Hydbring, P., Malumbres, M. & Sicinski, P. Non-canonical functions of cell cycle cyclins and cyclin-dependent kinases. *Nat. Rev. Mol. Cell Biol.* **17**, 280–292 (2016).
47. Narasimha, A. M. *et al.* Cyclin D activates the Rb tumor suppressor by mono-phosphorylation. *Elife* **3**, (2014).
48. Coverley, D., Laman, H. & Laskey, R. A. Distinct roles for cyclins E and A during DNA replication complex assembly and activation. *Nat. Cell Biol.* **4**, 523–528 (2002).
49. Sherr, C. J. & Roberts, J. M. CDK inhibitors: positive and negative regulators of G1-phase progression. *Genes Dev.* **13**, 1501–1512 (1999).
50. Dyson, N. The regulation of E2F by pRB-family proteins. *Genes Dev.* **12**, 2245–2262 (1998).
51. Cheng, C.-W., Leong, K.-W., Ng, Y.-M., Kwong, Y.-L. & Tse, E. The peptidyl-prolyl isomerase PIN1 relieves cyclin-dependent kinase 2 (CDK2) inhibition by the CDK inhibitor p27. *J. Biol. Chem.* **292**, 21431–21441 (2017).
52. Bertoli, C., Skotheim, J. M. & de Bruin, R. A. M. Control of cell cycle transcription during G1 and S phases. *Nat. Rev. Mol. Cell Biol.* **14**, 518–528 (2013).
53. Barr, A. R. *et al.* DNA damage during S-phase mediates the proliferation-quiescence decision in the subsequent G1 via p21 expression. *Nat. Commun.* **8**, (2017).
54. Carey, B. W., Finley, L. W. S., Cross, J. R., Allis, C. D. & Thompson, C. B. Intracellular α-ketoglutarate maintains the pluripotency of embryonic stem cells. *Nature* **518**, 413–416 (2015).
55. Coronado, D. *et al.* A short G1 phase is an intrinsic determinant of naïve embryonic stem cell pluripotency. *Stem Cell Res.* **10**, 118–131 (2013).
56. ter Huurne, M., Chappell, J., Dalton, S. & Stunnenberg, H. G. Distinct Cell-Cycle Control in Two Different States of Mouse Pluripotency. *Cell Stem Cell* **21**, 449-455.e4 (2017).
57. White, J. *et al.* Developmental Activation of the Rb–E2F Pathway and Establishment of Cell Cycle-regulated Cyclin-dependent Kinase Activity during Embryonic Stem Cell Differentiation. *Mol. Biol. Cell* **16**, 2018–2027 (2005).
58. Fujii-Yamamoto, H., Kim, J. M., Arai, K. & Masai, H. Cell Cycle and Developmental Regulations of Replication Factors in Mouse Embryonic Stem Cells. *J. Biol. Chem.* **280**, 12976–12987 (2005).
59. Gonnot, F., Langer, D., Bourillot, P. Y., Doerflinger, N. & Savatier, P. Regulation of Cyclin E by transcription factors of the naïve pluripotency network in mouse embryonic stem cells. *Cell Cycle* **18**, 2697–2712 (2019).
60. Bar-On, O., Shapira, M., Skorecki, K., Hershko, A. & Hershko, D. D. Regulation of APC/CCdh1 ubiquitin ligase in differentiation of human embryonic stem cells. *Cell Cycle* **9**, 1986–1989 (2010).
61. Liu, L. *et al.* G1 cyclins link proliferation, pluripotency and differentiation of embryonic stem cells. *Nat. Cell Biol.* **19**, 177–188 (2017).
62. Ouyang, J. *et al.* Cyclin-dependent Kinase-mediated Sox2 Phosphorylation Enhances the Ability of Sox2 to Establish the Pluripotent State. *J. Biol. Chem.* **290**, 22782–22794 (2015).
63. Solozobova, V. & Blattner, C. Regulation of p53 in embryonic stem cells. *Exp. Cell Res.* **316**, 2434–2446 (2010).
64. Aladjem, M. I. *et al.* ES cells do not activate p53-dependent stress responses and undergo p53-independent apoptosis in response to DNA damage. *Curr. Biol.* **8**, 145–155 (1998).
65. Suvorova, I. I., Grigorash, B. B., Chuykin, I. A., Pospelova, T. V. & Pospelov, V. A. G1 checkpoint is compromised in mouse ESCs due to functional uncoupling of p53-p21Waf1 signaling. *Cell Cycle* **15**, 52–63 (2016).
66. Malashicheva, A. B., Kislyakova, T. V, Aksenov, N. D., Osipov, K. A. & Pospelov, V. A. F9 embryonal carcinoma cells fail to stop at G1/S boundary of the cell cycle after γ-irradiation due to p21WAF1/CIP1 degradation. *Oncogene* **19**, 3858–3865 (2000).
67. Rehman, S. K. *et al.* Colorectal Cancer Cells Enter a Diapause-like DTP State to Survive Chemotherapy. *Cell* **184**, 226-242.e21 (2021).
68. Hooper, M., Hardy, K., Handyside, A., Hunter, S. & Monk, M. HPRT-deficient (Lesch–Nyhan) mouse embryos derived from germline colonization by cultured cells. *Nature* **326**, 292–295 (1987).

69. SHERMAN, M. I. & BARLOW, P. W. DEOXYRIBONUCLEIC ACID CONTENT IN DELAYED MOUSE BLASTOCYSTS. *Reproduction* **29**, 123–126 (1972).
70. Given, R. L. DNA synthesis in the mouse blastocyst during the beginning of delayed implantation. *J. Exp. Zool.* **248**, 365–70 (1988).
71. TM, M. Changes in mouse blastocyst carbon dioxide production as a function of time postcoitum in delay of implantation during lactation or following ovariectomy. *Biol Reprod* **7**, 414–416 (1972).
72. Hamatani, T. *et al.* Global gene expression analysis identifies molecular pathways distinguishing blastocyst dormancy and activation. *Proc. Natl. Acad. Sci. U. S. A.* **101**, 10326–31 (2004).
73. Fry, D. W. *et al.* Specific inhibition of cyclin-dependent kinase 4/6 by PD 0332991 and associated antitumor activity in human tumor xenografts. *Mol. Cancer Ther.* **3**, 1427–38 (2004).
74. Jirawatnotai, S., Dalton, S. & Wattanapanitch, M. Role of cyclins and cyclin-dependent kinases in pluripotent stem cells and their potential as a therapeutic target. *Semin. Cell Dev. Biol.* **107**, 63–71 (2020).
75. Bollard, J. *et al.* Palbociclib (PD-0332991), a selective CDK4/6 inhibitor, restricts tumour growth in preclinical models of hepatocellular carcinoma. *Gut* **66**, 1286–1296 (2017).
76. Khoa, L. T. P. *et al.* Histone Acetyltransferase MOF Blocks Acquisition of Quiescence in Ground-State ESCs through Activating Fatty Acid Oxidation. *Cell Stem Cell* **27**, 441-458.e10 (2020).
77. Young, A. R. J., Narita, M. & Narita, M. Cell Senescence as Both a Dynamic and a Static Phenotype. in 1–13 (2013). doi:10.1007/978-1-62703-239-1_1.
78. Stead, E. *et al.* Pluripotent cell division cycles are driven by ectopic Cdk2, cyclin A/E and E2F activities. *Oncogene* **21**, 8320–8333 (2002).
79. Berrill, A. *et al.* Assessment of Stem Cell Markers During Long-Term Culture of Mouse Embryonic Stem Cells. *Cytotechnology* **44**, 77–91 (2004).
80. Malinowski, A. The contribution of the cell cycle to reprogramming and the role of Jarid2 in coordinating Nanog expression and Wnt/PCP signalling in mESC differentiation and early development. *spiral.imperial.ac.uk* doi:https://doi.org/10.25560/58229.
81. Portman, N. *et al.* Overcoming CDK4/6 inhibitor resistance in ER-positive breast cancer. *Endocr. Relat. Cancer* **26**, R15–R30 (2019).
82. Hai, J. *et al.* Synergy of WEE1 and mTOR Inhibition in Mutant KRAS -Driven Lung Cancers. *Clin. Cancer Res.* **23**, 6993–7005 (2017).
83. Sun, X. *et al.* DICER1 regulated let-7 expression levels in p53-induced cancer repression requires cyclin D1. *J. Cell. Mol. Med.* **19**, 1357–1365 (2015).
84. Stallaert, W. *et al.* The structure of the human cell cycle. *Cell Syst.* **37**, 43–6 (2021).
85. T., L. C. and R. F. and B. L. M. and R. H. W. and A. C. and C. S. and T. L. and J. G. C. and A. CDK4/6 inhibitors induce replication stress to cause long-term cell cycle Saurin. *bioRxiv* (2021).
86. Spencer, S. L. *et al.* The Proliferation-Quiescence Decision Is Controlled by a Bifurcation in CDK2 Activity at Mitotic Exit. *Cell* **155**, 369–383 (2013).
87. Henley, S. A. & Dick, F. A. The retinoblastoma family of proteins and their regulatory functions in the mammalian cell division cycle. *Cell Div.* **7**, 10 (2012).
88. Xiong, Y., Zhang, H. & Beach, D. D type cyclins associate with multiple protein kinases and the DNA replication and repair factor PCNA. *Cell* **71**, 505–14 (1992).
89. Wang, L. *et al.* Pharmacologic inhibition of CDK4/6: mechanistic evidence for selective activity or acquired resistance in acute myeloid leukemia. *Blood* **110**, 2075–83 (2007).
90. Dean, J. L., Thangavel, C., McClendon, A. K., Reed, C. A. & Knudsen, E. S. Therapeutic CDK4/6 inhibition in breast cancer: key mechanisms of response and failure. *Oncogene* **29**, 4018–32 (2010).
91. Lin, R. *et al.* 1-Acyl-1 H -[1,2,4]triazole-3,5-diamine Analogues as Novel and Potent Anticancer Cyclin-Dependent Kinase Inhibitors: Synthesis and Evaluation of Biological Activities. *J. Med. Chem.* **48**, 4208–4211 (2005).
92. Knudsen, E. S. & Witkiewicz, A. K. Defining the transcriptional and biological response to CDK4/6 inhibition in relation to ER+/HER2- breast cancer. *Oncotarget* **7**, 69111–69123 (2016).
93. Michaloglou, C. *et al.* Combined Inhibition of mTOR and CDK4/6 Is Required for Optimal Blockade of E2F Function and Long-term Growth Inhibition in Estrogen Receptor–positive

Breast Cancer. *Mol. Cancer Ther.* **17**, 908–920 (2018).
94. Lin, T. *et al.* p53 induces differentiation of mouse embryonic stem cells by suppressing Nanog expression. *Nat. Cell Biol.* **7**, 165–171 (2005).
95. Solozobova, V. & Blattner, C. Regulation of p53 in embryonic stem cells. *Exp. Cell Res.* **316**, 2434–46 (2010).
96. Martello, G. & Smith, A. The Nature of Embryonic Stem Cells. *Annu. Rev. Cell Dev. Biol.* **30**, 647–675 (2014).
97. Mulas, C. *et al.* Correction: Defined conditions for propagation and manipulation of mouse embryonic stem cells (doi:10.1242/dev.173146). *Dev.* **146**, (2019).
98. Toogood, P. L. *et al.* Discovery of a Potent and Selective Inhibitor of Cyclin-Dependent Kinase 4/6. *J. Med. Chem.* **48**, 2388–2406 (2005).
99. Carvajal, D. *et al.* Activation of p53 by MDM2 Antagonists Can Protect Proliferating Cells from Mitotic Inhibitors. *Cancer Res.* **65**, 1918–1924 (2005).
100. Secchiero, P. *et al.* Antiangiogenic Activity of the MDM2 Antagonist Nutlin-3. *Circ. Res.* **100**, 61–69 (2007).
101. Tesar, P. J. *et al.* New cell lines from mouse epiblast share defining features with human embryonic stem cells. *Nature* **448**, 196–9 (2007).
102. Huang, K., Maruyama, T. & Fan, G. The Naive State of Human Pluripotent Stem Cells: A Synthesis of Stem Cell and Preimplantation Embryo Transcriptome Analyses. *Cell Stem Cell* **15**, 410–415 (2014).
103. Stirparo, G. G. *et al.* Integrated analysis of single-cell embryo data yields a unified transcriptome signature for the human preimplantation epiblast. *Development* (2018) doi:10.1242/dev.158501.
104. Dodsworth, B. T. *et al.* Profiling of naïve and primed human pluripotent stem cells reveals state-associated miRNAs. *Sci. Rep.* **10**, 10542 (2020).
105. Schade, A. E., Oser, M. G., Nicholson, H. E. & DeCaprio, J. A. Cyclin D–CDK4 relieves cooperative repression of proliferation and cell cycle gene expression by DREAM and RB. *Oncogene* **38**, 4962–4976 (2019).
106. Yang, P. *et al.* Downregulation of cyclin D1 sensitizes cancer cells to MDM2 antagonist Nutlin-3. *Oncotarget* **7**, 32652–32663 (2016).
107. Kan, C. E., Patton, J. T., Stark, G. R. & Jackson, M. W. p53-Mediated Growth Suppression in Response to Nutlin-3 in Cyclin D1–Transformed Cells Occurs Independently of p21. *Cancer Res.* **67**, 9862–9868 (2007).
108. Lin, Y.-H. & Zhu, H. A Malignant Case of Arrested Development: Cancer Cell Dormancy Mimics Embryonic Diapause. *Cancer Cell* **39**, 142–144 (2021).

7. Supplements

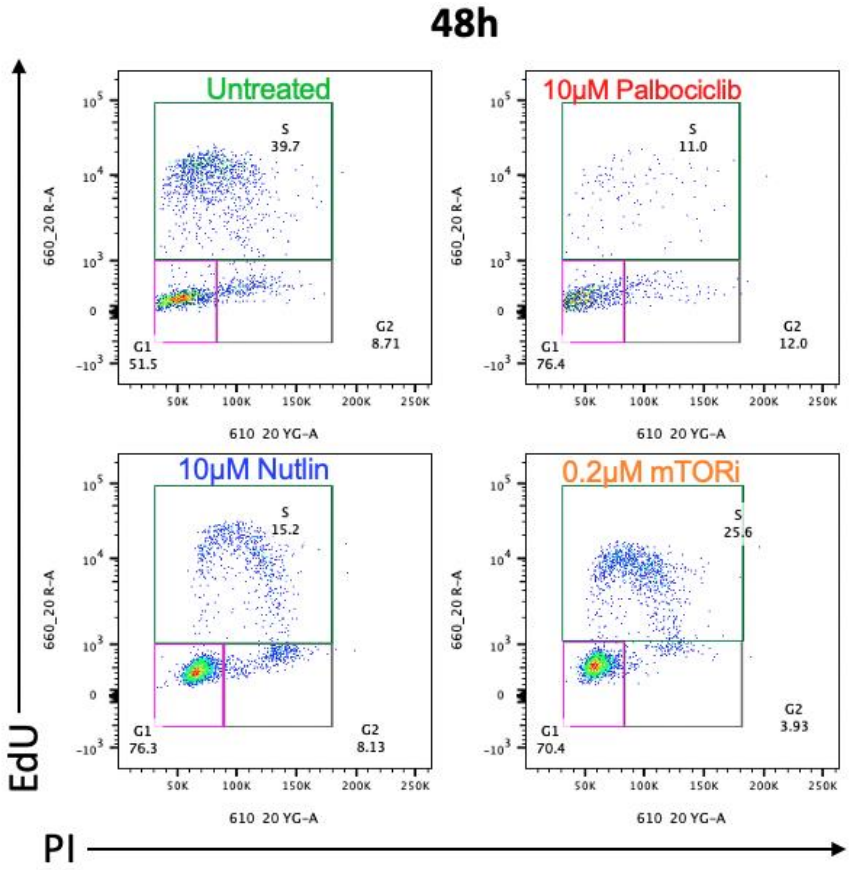

Figure S3-1 ***FACS graph plots from 48h treated cells.*** *Cells were seeded and after 24h treated with respective condition. After 48h, cells were pulsed for EdU, fixed, stained for EdU and PI and analysed by flow cytometry. The percentage of cells in phase obtained from the Flow cytometry analysis of mESCs treated for 48h with all conditions, were plotted by Flow Jo.*

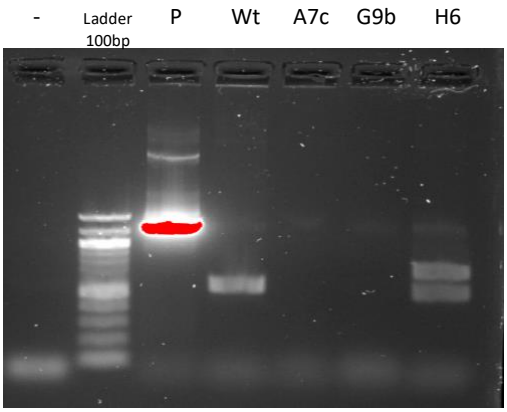

Figure S3-2- ***Confirmation of the results from the PCR of H6.*** *1% of agarose gel electrophoresis of PCR products for Cdkn1a primers. (-) lane refers to the negative control performed with H2O; P is PCR product against plasmid DNA (plasmid with p21 homologous regions and mRuby DNA); Wt refers to genomic DNA from untransfected E14 cells resultant from the PCR. A 100bp ladder was loaded in both lanes called "ladder". Other lanes are the PCR product from the PCR against the Clones genomic DNA.*